Efficient Approach to Solving Transient Unsaturated Flow Problems. I: Analytical Solutions

André Luís Brasil Cavalcante, Ph.D.[1]; and Jorge Gabriel Zornberg, Ph.D.[2]

Abstract: Richard's equation governs the migration of moisture in the soil under unsaturated conditions. Although this differential equation provides a rigorous approach to simulating important infiltration problems, obtaining analytical and numerical solutions to this equation has been a particularly challenging task. This is largely due to the highly nonlinear nature of the soil hydraulic properties, including the moisture retention curve and the hydraulic conductivity function. Whereas analytical solutions of Richard's equation have been reported for problems involving steady-state conditions and simple hydraulic models, solutions for transient conditions have rarely been obtained. However, such analytical solutions would be particularly valuable, for example, to validate the accuracy of numerical schemes, as well as to facilitate parametric evaluations. A series of analytical solutions of Richard's equation for unsaturated flow under transient conditions have been developed as part of this study. The solutions involve a variety of initial and boundary conditions. The analytical solutions in this study could be obtained after expressing the governing equation as the addition of advective and diffusive flow components. The solutions consider logarithmic and linear models to represent the soil moisture retention and the hydraulic conductivity functions, respectively. Solutions are also provided for special cases in which either the advective or the diffusive components dominate the flow process, as well as for the steady-state cases. A parametric evaluation was found to provide insight into important characteristics of infiltration problems. In particular, relevant features of an unsaturated flow problem can be explained by evaluating the trends in its advective and diffusive flow components. **DOI: 10.1061/(ASCE)GM.1943-5622.0000875.**

Author keywords: Unsaturated flow; Richard's equation; Analytical model; Advection; Diffusion.

Introduction

Richard's equation, which governs the migration of moisture in the soil under unsaturated conditions, results after assuming the validity of Darcy's law and continuity of flow. Although this partial differential equation represents a rigorous approach to simulate important infiltration problems, analytical solutions to Richard's equation have been particularly challenging to obtain. This is largely due to the highly nonlinear nature of the hydraulic properties of unsaturated soils, including the moisture retention curve and the hydraulic conductivity function.

Although analytical solutions of Richard's equation have been reported for problems involving steady-state conditions and simple hydraulic models, analytical solutions for transient conditions have usually required the use of approximate approaches that incorporated simplified assumptions (Philip 1960; Sander et al. 1988; Hogarth et al. 1989, 1992; Parlance et al. 1992; Parlange et al. 1997; Ross and Parlange 1994; Hogarth and Parlange 2000; Dell'Avanzi et al. 2004; Rathie et al. 2012; Cavalcante et al. 2013; Swamee et al. 2014). In the few reported studies in which exact solutions for transient conditions have been provided, the equations were presented using integral forms, which generally require the use of numerical approaches for their use (Wang and Dooge 1994; Basha 1999; Chen et al. 2001, 2003). Obtaining closed-form solutions to Richard's equation would be particularly valuable to (1) facilitate parametric evaluations, and (2) validate the accuracy of numerical schemes by allowing comparisons between analytical solutions and numerical predictions.

This paper presents the development of a series of analytical solutions to Richard's equation for unsaturated flow problems under transient conditions. The solutions involve a variety of boundary conditions, including imposing a constant moisture content to the upper boundary of a soil column (semi-infinite and finite-length cases) as well as imposing a constant discharge velocity to the upper boundary of a soil column (semi-infinite and finite-length cases).

As is presented in the paper, the analytical solutions obtained in this study could be derived after expressing the governing equation as the addition of advective and diffusive flow components. In fact, the proposed formulation allows the study of problems where the advective and diffusive flow components are coupled, as well as problems that can be simplified if the flow process is dominated by only one of the two flow components. Solutions are also provided for the steady-state cases.

General Framework for Solving Richard's Equation

The three-dimensional (3D) partial differential equation describing unsaturated, transient flow under a natural gravitational field can be derived by considering the validity of Darcy-Buckingham's law and the conservation of mass.

The mass inflow rate of fluids (e.g., water) [$\dot{m}_{in}$ (MT^{-1})] into a representative elementary volume (REV) with dimensions dx, dy, and dz can be represented as

[1]Associate Professor, Dept. of Civil and Environmental Engineering, Univ. of Brasília, Brasília-DF 70910-900, Brazil (corresponding author). ORCID: http://orcid.org/0000-0002-7104-0371. E-mail: abrasil@unb.br

[2]Professor, Dept. of Civil Architectural and Environmental Engineering, Univ. of Texas, Austin, TX 78712-0280. E-mail: zornberg@mail.utexas.edu

Note. This manuscript was submitted on April 9, 2016; approved on November 4, 2016; published online on February 6, 2017. Discussion period open until July 6, 2017; separate discussions must be submitted for individual papers. This paper is part of the ***International Journal of Geomechanics***, © ASCE, ISSN 1532-3641.

$$\dot{m}_{\text{in}} = v_x \rho_w (dzdy) + v_y \rho_w (dxdz) + v_z \rho_w (dxdy) \tag{1}$$

where ρ_w = fluid density (ML^{-3}); and v_x, v_y, and v_z = discharge velocities in the x-, y-, and z-directions (LT^{-1}), respectively. Also, the total mass outflow rate leaving the REV [$\dot{m}_{\text{out}}$ (MT^{-1})], can be represented as

$$\dot{m}_{\text{out}} = \left[\rho_w v_x + \frac{\partial(\rho_w v_x)}{\partial x} dx\right] dzdy + \left[\rho_w v_y + \frac{\partial(\rho_w v_y)}{\partial y} dy\right] dxdz + \left[\rho_w v_z + \frac{\partial(\rho_w v_z)}{\partial z} dz\right] dxdy \tag{2}$$

The rate of change in water storage within the REV [$\dot{m}_{\text{storage}}$ (MT^{-1})], is given by

$$\dot{m}_{\text{storage}} = \frac{\partial(\rho_w \theta)}{\partial t} dxdydz \tag{3}$$

where θ = volumetric water content (L^3L^{-3}); and t = time (T).

For fluids that are incompressible (i.e., ρ_w constant in time) and homogeneous (i.e., ρ_w constant in space), the continuity principle implies that the difference between the mass inflow and outflow rates should equal the rate of change in water volume storage. Using Eqs. (1)–(3), this principle results in

$$\frac{\partial \theta}{\partial t} = -\frac{\partial v_x}{\partial x} - \frac{\partial v_y}{\partial y} - \frac{\partial v_z}{\partial z} \tag{4}$$

The flow rate per unit of area (discharge velocity) in each direction can be defined using Darcy-Buckingham's law (Buckingham 1907; Narasimhan 2004), which is the unsaturated version of Darcy's law, as follows:

$$v_x = -\frac{k_x(\psi)}{g}\frac{\partial \Phi}{\partial x} \tag{5}$$

$$v_y = -\frac{k_y(\psi)}{g}\frac{\partial \Phi}{\partial y} \tag{6}$$

$$v_z = -\frac{k_z(\psi)}{g}\frac{\partial \Phi}{\partial z} \tag{7}$$

where ψ = soil suction (using atmospheric pressure as reference) ($ML^{-1}T^{-2}$); and $k_x(\psi)$, $k_y(\psi)$, and $k_z(\psi)$ = hydraulic conductivity functions (k-functions) expressed in terms of ψ in the x-, y-, and z-directions (LT^{-1}), respectively. The variable Φ corresponds to the fluid potential (i.e., energy per unit mass of fluid) in the REV, which is defined as

$$\Phi = -gz + \frac{\psi}{\rho_w} \tag{8}$$

where g = acceleration of gravity (LT^{-2}); and z = elevation above a datum (L).

Considering Eq. (8) in Eqs. (5)–(7), the discharge velocity in each direction can be rewritten as

$$v_x = \frac{k_x(\psi)}{\rho_w g}\frac{\partial \psi}{\partial x} \tag{9}$$

$$v_y = \frac{k_y(\psi)}{\rho_w g}\frac{\partial \psi}{\partial y} \tag{10}$$

$$v_z = \frac{k_z(\psi)}{\rho_w g}\frac{\partial \psi}{\partial z} - k_z(\psi) \tag{11}$$

It should be noted that, as reported by Biot (1941), the continuity equation for water is expressed in terms of absolute velocities [Eq. (4)]. However, Darcy-Buckingham's law [Eqs. (9)–(11)] uses relative velocities of water (in relation to the solid particles). Consequently, an implicit assumption made in the formulation presented herein is that the solid particles do not move (i.e., relative water velocities equal the absolute velocities). This assumption, also adopted by Terzaghi (1943) along with multiple other formulations, has been found to be satisfactory for most geotechnical applications.

It should be noted that the formulation solved analytically in the paper does not address volumetric changes, which are particularly relevant in unsaturated soil mechanics. Important problems that are beyond the scope of this paper include, for example, metastable soil structures that collapse as a result of a gradual reduction in matric suction, soils with a stable structure that swell when the matric suction decreases, and the hysteretic response of water retention.

The formulation presented in this paper assumes that the flow of water occurs in an unsaturated porous medium where the volumetric changes are negligible. Consequently, the soil porosity can be considered constant. This behavior is common in cemented soils developed in arid to subhumid climates.

Considering Eqs. (9)–(11) into Eq. (4) leads to the 3D version of Richard's equation unsaturated transient flow, as follows:

$$\frac{\partial \theta}{\partial t} = \frac{\partial}{\partial x}\left[\frac{k_x(\psi)}{\rho_w g}\frac{\partial \psi}{\partial x}\right] + \frac{\partial}{\partial y}\left[\frac{k_y(\psi)}{\rho_w g}\frac{\partial \psi}{\partial y}\right] + \frac{\partial}{\partial z}\left[k_z(\psi)\left(\frac{1}{\rho_w g}\frac{\partial \psi}{\partial z} - 1\right)\right] \tag{12}$$

Accordingly, the model presented in Eq. (12) assumes that all changes in θ occur in the water retention due to changes in the degree of saturation (i.e., the porosity of the soil remains essentially constant during any wetting/drying paths). Because the model presented in this study is one-dimensional, it applies, for example, to experimental column tests, where the porosity of the soil remains constant during the test.

Because θ and ψ in Eq. (12) are dependent variables, it is more convenient to express this equation in terms of either $\psi = f(\theta)$ or $\theta = f^{-1}(\psi)$. In this paper, the differential equation is solved using θ as an independent variable. As is subsequently discussed, the unsaturated flow differential equation that results after adopting θ as an independent variable can be ultimately presented using terms that are analogous to those of the advection-dispersion contaminant transport differential equation. This analogy is convenient, as analytical solutions (for simple initial and boundary conditions) as well as well-established numerical schemes (for more complex conditions) have been studied for the advection-dispersion equation.

The use of θ as an independent variable can be achieved by replacing $\partial\psi/\partial x$, $\partial\psi/\partial y$, and $\partial\psi/\partial z$ with $(\partial\psi/\partial\theta)(\partial\theta/\partial x)$, $(\partial\psi/\partial\theta)(\partial\theta/\partial y)$, and $(\partial\psi/\partial\theta)(\partial\theta/\partial z)$, respectively, in Eq. (12). The resulting equation can be expressed using the unsaturated water diffusivity [D_x, D_y, and D_z (L^2T^{-1})], which can be defined as

$$D_x(\theta) = \frac{k_x(\theta)}{\rho_w g}\frac{\partial \psi}{\partial \theta} \tag{13}$$

$$D_y(\theta) = \frac{k_y(\theta)}{\rho_w g}\frac{\partial \psi}{\partial \theta} \tag{14}$$

$$D_z(\theta) = \frac{k_z(\theta)}{\rho_w g}\frac{\partial \psi}{\partial \theta} \tag{15}$$

where $k_x(\theta)$, $k_y(\theta)$, and $k_z(\theta)$ = hydraulic conductivity functions (k-functions) expressed in terms of θ in the x-, y-, and z-directions (LT^{-1}); and the term $\partial\psi/\partial\theta$, which has often been defined as the specific water capacity, is the reciprocal of the slope of the soil water retention curve (SWRC). The specific water capacity is highly sensitive to the soil type, soil placement conditions, and wetting path. The specific water capacity ranges from $-\infty$ (i.e., a vertical trend in the SWRC) to 0 (i.e., a horizontal trend).

Using Eqs. (13)–(15) in Eq. (12), the following θ-based version of Richard's equation can then be obtained

$$\frac{\partial \theta}{\partial t} = \frac{\partial}{\partial x}\left[D_x(\theta)\frac{\partial \theta}{\partial x}\right] + \frac{\partial}{\partial y}\left[D_y(\theta)\frac{\partial \theta}{\partial y}\right] + \frac{\partial}{\partial z}\left[D_z(\theta)\frac{\partial \theta}{\partial z}\right] - \frac{\partial k_z(\theta)}{\partial z} \tag{16}$$

Eq. (16) can referred to as the Fokker-Planck equation (Philip 1969; Bear 1979). For the case of a one-dimensional unsaturated flow in the z-direction, Eq. (16) results in

$$\frac{\partial \theta}{\partial t} = \frac{\partial}{\partial z}\left[D_z(\theta)\frac{\partial \theta}{\partial z}\right] - \frac{\partial k_z(\theta)}{\partial z} \tag{17}$$

Eq. (17) is the one-dimensional, θ-based Richard's equation. In this paper, a more convenient form of this equation is used, which is obtained by replacing $\partial k_z/\partial z$ with $(\partial k_z/\partial\theta)(\partial\theta/\partial z)$ in Eq. (17) as follows:

$$\frac{\partial \theta}{\partial t} = \frac{\partial}{\partial z}\left[D_z(\theta)\frac{\partial \theta}{\partial z}\right] - a_s(\theta)\frac{\partial \theta}{\partial z} \tag{18}$$

where

$$a_s(\theta) = \frac{\partial k_z(\theta)}{\partial \theta} \tag{19}$$

where $a_s(\theta)$ = unsaturated advective seepage. Physically, $a_s(\theta)$ corresponds to the slope of the k-function when expressed in terms of θ (Fig. 1), and consequently, it has units of velocity (LT^{-1}).

A benefit of solving Richard's equation using θ as the independent variable is that the unsaturated water diffusivity (D_z) does not vary with θ nearly as much as the unsaturated hydraulic conductivity (k_z) varies with ψ. In addition, the function expressing the hydraulic conductivity in terms of volumetric water content ($k_z(\theta)$) has been reported to show less hysteresis, if any, than the $k_z(\psi)$ function (Hillel 2004). A potential disadvantage of this approach is that its implementation may be more problematic to simulating flow in soils with a high degree of saturation because D_z tends to infinity under saturated conditions (i.e., $\partial\theta/\partial\psi$ tends to 0). However, an additional important advantage of adopting θ as the independent variable and using the unsaturated advective seepage [$a_s(\theta)$] is that the resulting Eq. (18) is analogous to the advection-dispersion contaminant transport differential equation. Accordingly, the terms in Eq. (18) can be thought of as corresponding to advective and diffusive components of an unsaturated flow process. The advective component corresponds to the flow of water advancing via gravitational, advective-like (bulk) motion within the porous medium. In contrast, the diffusive component corresponds to flow of water spreading in a (diffusive-like) motion. Because Eq. (18) involves three unknowns (θ, k_z, and ψ), its solution requires two additional relationships. These relationships have often been established experimentally to define, for example, the unsaturated hydraulic conductivity (k_z) and the volumetric water content (θ) in terms of suction (ψ).

Considering the analogy that can be established between Eq. (18) and the advection-dispersion contaminant transport equation, the overall unsaturated flow can be grouped into advective and diffusive flow components (Appendix I). Advective flow corresponds to the unsaturated flow component that is driven by gravitational (or potential) energy, as follows:

$$f_{adv}(z,t) = a_s(\theta)\cdot\theta \tag{20}$$

where f_{adv} = advective flow component of the overall unsaturated flow process (LT^{-1}). In contrast, the diffusive flow corresponds to the spreading of moisture that is driven by gradients in volumetric water content (and, consequently, by gradients in suction). This can be represented as follows:

$$f_{dif}(z,t) = -D_z(\theta)\frac{\partial \theta}{\partial z} \tag{21}$$

where f_{dif} = diffusive flow component of the overall unsaturated flow process (LT^{-1}).

Analytical Solutions of Transient Unsaturated Flow Problems

A limited number of closed-form analytical solutions to the highly nonlinear Richard's equation have been reported in the literature. Solutions for transient condition problems have used integral forms, which generally require numerical approaches for their implementation [e.g., Fityus and Smith (2001); Ghotbi et al. (2011); Huang and Wu (2012)]. The majority of the reported solutions have been for cases involving the much simpler steady-state conditions [e.g., Gardner (1958); Yeh (1989); Tartakovsky et al. (1999); Zhu and Mohanty (2002); Chen and Gallipoli (2004); Dell'Avanzi et al. (2004)].

In this paper, analytical closed-form solutions were developed for Richard's equation for the case of transient flow conditions. This was achieved by adopting particular relationships to represent

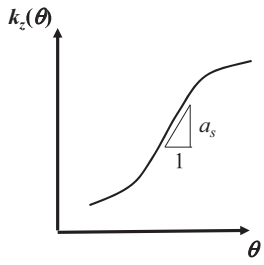

Fig. 1. Physical interpretation of unsaturated advective seepage [$a_s(\theta)$]

the SWRC and k-function in the general unsaturated flow framework expressed by Eq. (18). Specifically, the adopted hydraulic functions involve a logarithmic relationship between suction and volumetric water content [$\psi(\theta)$] and a linear relationship between unsaturated hydraulic conductivity and volumetric water content [$k_z(\theta)$]. Accordingly, $\psi(\theta)$ is represented by

$$\psi(\theta) = \frac{1}{\delta} \ln\left(\frac{\theta - \theta_r}{\theta_s - \theta_r}\right) \tag{22}$$

where θ_s = volumetric water content at saturation (L^3/L^3); θ_r = residual volumetric water content (L^3/L^3); and δ = fitting hydraulic parameter ($M^{-1}LT^2$). The difference between θ_s and θ_r has often been referred to as the soil moisture capacity. In contrast, the unsaturated hydraulic conductivity [$k_z(\theta)$] is represented by

$$k_z(\theta) = k_s\left(\frac{\theta - \theta_r}{\theta_s - \theta_r}\right) \tag{23}$$

where k_s = saturated hydraulic conductivity of the soil (L/T).

Fig. 2(a) illustrates the effect of varying the hydraulic parameter δ on the SWRC represented by Eq. (22), whereas Fig. 2(b) shows the effect of varying the parameter δ on the k-function represented by Eq. (23). The curves in Fig. 2 were generated using values of 0.3, 0.03, and 0.003 kPa^{-1} for the hydraulic parameter δ. The parameters θ_r, θ_s, and k_s adopted for the curves in this figure are 0.04, 0.41, and 8.2×10^{-7} m/s, respectively. The results in Fig. 2 illustrate that

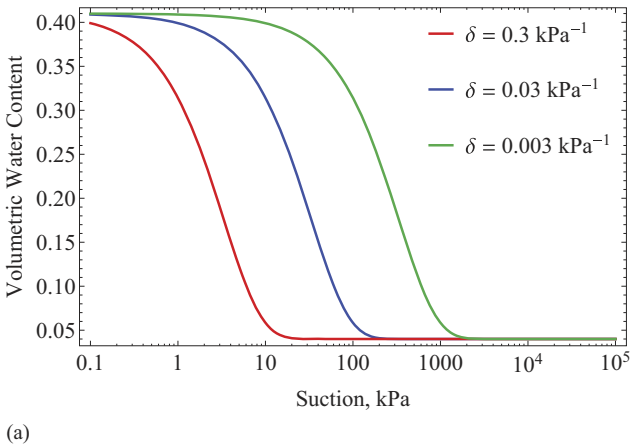

(a)

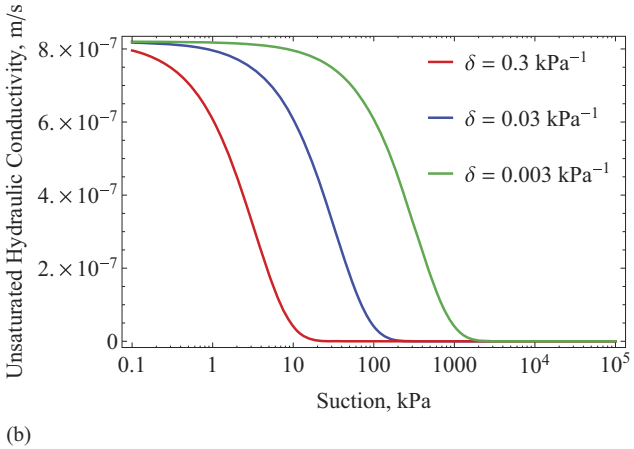

(b)

Fig. 2. (Color) Sensitivity of hydraulic parameter (δ): (a) SWRC; (b) k-function ($\theta_r = 0.04$, $\theta_s = 0.41$, and $k_s = 8.2 \times 10^{-7}$ m/s)

the magnitude of parameter δ significantly affects the air-entry pressure of the soil.

It can be demonstrated (Appendix II) that the hydraulic parameter δ is proportional to the initial slope of the SWRC (i.e., the slope at saturation). Fig. 3 illustrates the physical interpretation of parameters θ_r, θ_s, and δ on the SWRC.

Aditionally, it can be demonstrated (Appendix II) that the hydraulic parameter δ is also proportional to the initial slope of the k-function (i.e., the slope at saturation). Fig. 4 illustrates the physical interpretation of parameters k_s and δ on the k-function.

An important consequence of adopting the unsaturated hydraulic relationships represented by Eqs. (22) and (23) is that the hydraulic parameters $D_z(\theta)$ [Eq. (15)] and $a_s(\theta)$ [Eq. (19)] become constants. Specifically, the resulting hydraulic parameters are

$$\bar{D}_z = \frac{k_s}{\delta(\theta_s - \theta_r)\rho_w g} \tag{24}$$

$$\bar{a}_s = \frac{k_s}{(\theta_s - \theta_r)} \tag{25}$$

where $\bar{D}_z$ = constant unsaturated water diffusivity in the z-direction; and $\bar{a}_s$ = constant unsaturated advective seepage, as obtained when

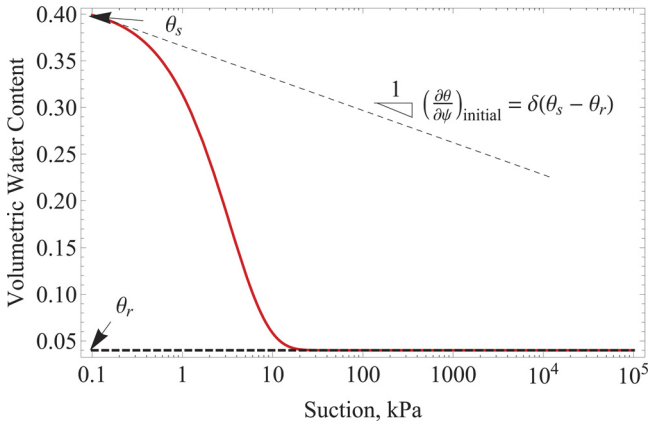

Fig. 3. (Color) Physical representation of parameters δ, θ_s, and θ_r in a SWRC ($\delta = 0.3\ kPa^{-1}$, $\theta_s = 0.41$, $\theta_r = 0.04$)

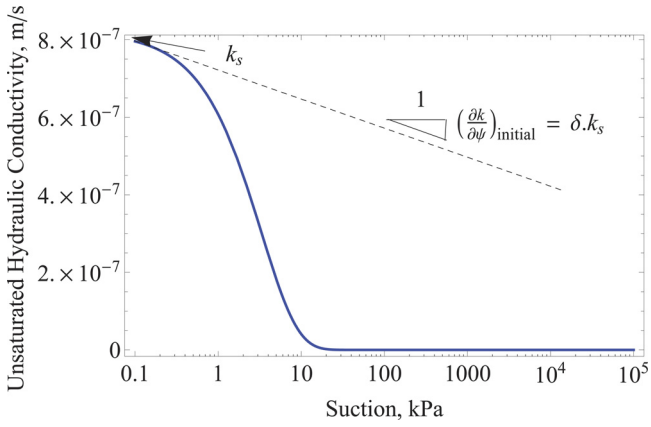

Fig. 4. (Color) Physical representation of parameters δ and k_s in a k-function ($\delta = 0.3\ kPa^{-1}$, $k_s = 8.2 \times 10^{-7}$ m/s)

$\psi(\theta)$ and $k_z(\theta)$ are represented by logarithmic and linear relationships, respectively.

For the adopted hydraulic relationships [Eqs. (22) and (23)], Richard's equation [Eq. (18)] can then be represented as

$$\frac{\partial\theta}{\partial t} = \bar{D}_z \frac{\partial^2\theta}{\partial z^2} - \bar{a}_s \frac{\partial\theta}{\partial z} \tag{26}$$

For steady-state conditions, Eq. (26) becomes

$$\bar{D}_z \frac{d^2\theta}{dz^2} - \bar{a}_s \frac{d\theta}{dz} = 0 \tag{27}$$

In summary, the general framework for unsaturated flow evaluated in this study is represented by Eq. (18) for the general case, where $D_z(\theta)$ and $a_s(\theta)$ are (often highly nonlinear) functions of θ. In contrast, a general unsaturated flow problem results in a much simpler one represented by Eq. (26), where $\bar{D}_z$ and $\bar{a}_s$ are constant values. A notable characteristic of Eq. (26) is its analogy to the advection-dispersion contaminant transport equation

$$\frac{\partial c}{\partial t} = D_h \frac{\partial^2 c}{\partial z^2} - v_s \frac{\partial c}{\partial z} \tag{28}$$

where c = concentration of a solute (ML^{-3}) as a function of space (z) and time (t). As in the case of Eq. (26), the relevant parameters in Eq. (28) are constants. Specifically, the constant D_h is the coefficient of longitudinal hydrodynamic dispersion (L^2/T), and the constant v_s is the average linear velocity (L/T).

Mathematical techniques previously used to solve the advection-diffusion equation with constant parameters (e.g., Fourier series, Laplace transformations) were used in this study to solve the unsaturated flow differential equation represented by Eq. (26). These techniques have been previously reported in the technical literature for the case of problems involving contaminant transport processes [e.g., Mason and Weaver (1924); Lapidus and Amundson (1952); Ogata and Banks (1961); Lindstrom et al. (1967); Gershon and Nir (1969); Cleary and Adrian (1973); Jaiswal et al. (2011); Cavalcante and Farias (2013)].

Solutions of one-dimensional transient infiltration problems require an initial and two boundary conditions. In this study, Eqs. (26) and (27) were analytically solved using Laplace transformations in the time domain for four cases involving different initial and boundary conditions. In each case, codes were developed using *Mathematica 10.0* to implement the analytical formulations.

Case 1: Imposed Constant Moisture to Upper Boundary of a Semi-infinite Column

This case involves solving for $\theta(z,t)$ considering an initial condition described by a uniform initial moisture content, as follows:

$$\theta(z,0) = \theta_i \tag{29}$$

where θ_i = constant. The Dirichlet boundary condition is adopted in this case, which involves a constant volumetric water content imposed at the upper boundary of the domain

$$\theta(0,t) = \theta_0 \tag{30}$$

where θ_0 = constant. For the semi-infinite domain, the lower boundary condition is described by

$$\frac{\partial\theta}{\partial z}(\infty,t) = 0 \tag{31}$$

This lower boundary condition implies that, at depth, the moisture content (and consequently, the suction) reaches a constant value. It also implies that, at depth, the hydraulic gradient in the z-direction equals 1. Solutions to partial differential equations involving these types of initial and boundary conditions have been reported for contaminant transport problems (Lapidus and Amundson 1952; Ogata and Banks 1961).

The analytical solution of Eq. (26) for these initial and boundary conditions was found to be

$$\theta(z,t) = \theta_i + (\theta_0 - \theta_i)A(z,t) \tag{32}$$

where

$$A(z,t) = \frac{1}{2}\left[\text{erfc}(Z_{-1}) + \exp\left(\frac{\bar{a}_s z}{\bar{D}_z}\right)\text{erfc}(Z_{+1})\right] \tag{33}$$

$$Z_{\pm 1} = \frac{z \pm \bar{a}_s t}{2\sqrt{\bar{D}_z t}} \tag{34}$$

where erfc(Z) = complementary error function, defined as follows:

$$\text{erfc}(Z) = 1 - \frac{2}{\pi}\int_0^Z \exp\left(-t^2\right)dt \tag{35}$$

In the particular case where $\bar{a}_s = 0$, the analytical solution of Eq. (26) for these initial and boundary conditions reduces to

$$\theta(z,t) = \theta_i + (\theta_0 - \theta_i)\text{erfc}\left(\frac{z}{2\sqrt{\bar{D}_z t}}\right) \tag{36}$$

Also, in the particular case where $\bar{D}_z = 0$, the analytical solution of Eq. (26) for these initial and boundary conditions reduces to

$$\theta(z,t) = \theta_i + (\theta_0 - \theta_i)H(\bar{a}_s t - z) \tag{37}$$

where $H(x)$ = Heaviside function, given by

$$H(\chi) = \begin{cases} 0, & \text{if } \chi \le 0 \\ 1, & \text{if } \chi > 0 \end{cases} \tag{38}$$

For the steady-state condition, Richard's equation is now represented by an ordinary differential equation [Eq. (27)]. Accordingly, flow problems can be solved by adopting only two boundary conditions (i.e., it is not necessary to establish an initial condition). The Dirichlet boundary condition adopted in this case (a constant volumetric water content imposed to the upper boundary of the domain) corresponds to

$$\theta(0) = \theta_0 \tag{39}$$

where θ_0 = constant. For the semi-infinite column, the lower boundary condition is described by

$$\frac{d\theta}{dz}(\infty) = 0 \tag{40}$$

The analytical solution for steady-state conditions using these boundary conditions is

$$\theta(z) = \theta_0 \tag{41}$$

Case 2: Imposed Constant Moisture to Upper Boundary of a Column of Finite Length

As in Case 1, the initial condition for Case 2 is also described by a uniform initial moisture content, as expressed by Eq. (29). Also as in Case 1, the Dirichlet boundary condition is adopted in Case 2, which involves a constant volumetric water content imposed to the upper boundary of the domain, as expressed by Eq. (30).

For a column of length L, the lower boundary condition was adopted to correspond to a zero gradient of the volumetric water content, which is expressed by

$$\frac{\partial \theta}{\partial z}(L,t) = 0 \tag{42}$$

As previously discussed, this lower boundary condition implies having a constant moisture content (and suction) at depth L, as well as having a unity hydraulic gradient at this depth. Solutions to partial differential equations with these types of initial and boundary conditions have been reported for contaminant transport problems (Cleary and Adrian 1973).

The analytical solution of Eq. (26) for these initial and boundary conditions was obtained as follows:

$$\theta(z,t) = \theta_i + (\theta_0 - \theta_i)B(z,t) \tag{43}$$

where

$$B(z,t) = 1 - \sum_{m=1}^{\infty} \frac{2\beta_m \sin\left(\frac{\beta_m z}{L}\right)\exp\left(\frac{\bar{a}_s z}{2\bar{D}_z} - \frac{\bar{a}_s^2 t}{4\bar{D}_z} - \frac{\beta_m^2 \bar{D}_z t}{L^2}\right)}{\left[\beta_m^2 + \frac{\bar{a}_s L}{2\bar{D}_z} + \left(\frac{\bar{a}_s L}{2\bar{D}_z}\right)^2\right]} \tag{44}$$

where β_m = eigenvalues corresponding to the positive roots of the equation

$$\beta_m \cot(\beta_m) + \frac{\bar{a}_s L}{2\bar{D}_z} = 0 \tag{45}$$

It is only necessary to consider approximately four terms of the series described by Eq. (44) to reach accurate results. In this case, Eq. (44) can be approximated by

$$\begin{aligned} B(z,t) = {} & \frac{1}{2}\mathrm{erfc}(Z_{-1}) + \frac{1}{2}\exp\left(\frac{\bar{a}_s z}{\bar{D}_z}\right)\mathrm{erfc}(Z_{+1}) \\ & + \frac{1}{2}\left[2 + \frac{\bar{a}_s(2L-z)}{\bar{D}_z} + \frac{\bar{a}_s^2 t}{\bar{D}_z}\right]\exp\left(\frac{\bar{a}_s L}{\bar{D}_z}\right) \\ & \times \mathrm{erfc}\left(\frac{2L - z + \bar{a}_s t}{2\sqrt{\bar{D}_z t}}\right) \\ & - \sqrt{\frac{\bar{a}_s^2 t}{\pi \bar{D}_z}}\exp\left[\frac{\bar{a}_s L}{\bar{D}_z} - \frac{(2L - z + \bar{a}_s t)^2}{4\bar{D}_z t}\right] \end{aligned} \tag{46}$$

In the particular case where $\bar{a}_s = 0$, the analytical solution of Eq. (26) for these initial and boundary conditions reduces to

$$\theta(z,t) = \theta_i + (\theta_0 - \theta_i)\left[1 + \sum_{m=1}^{\infty}\frac{4}{\pi}\sin\left(\frac{\pi z}{2L}\right)\exp\left(-\frac{\pi^2 \bar{D}_z t}{4L^2}\right)\right] \tag{47}$$

In this case, Eq. (45) has two roots ($\beta_m = \pm\pi/2$), but only the positive root gives a feasible solution. Considering approximately four terms of the series in Eq. (47), the following approximate expression can be obtained:

$$\theta(z,t) = \theta_i + (\theta_0 - \theta_i)\left[\mathrm{erfc}\left(\frac{z}{2\sqrt{\bar{D}_z t}}\right) + \mathrm{erfc}\left(\frac{2L - z}{2\sqrt{\bar{D}_z t}}\right)\right] \tag{48}$$

In the particular case where $\bar{D}_z = 0$, the analytical solution of Eq. (26) for these initial and boundary conditions reduces to Eq. (37), which is the same solution obtained for Case 1.

Also in this case, a steady-state solution can be obtained by solving Eq. (27). Specifically, the Dirichlet boundary condition is adopted in this case, as expressed by Eq. (39). For a column of length L, the adopted lower boundary condition corresponds to a zero volumetric water content gradient, which is expressed by

$$\frac{d\theta}{dz}(L) = 0 \tag{49}$$

The analytical solution for steady-state conditions using these boundary conditions was found to be the same as that obtained for Case 1 [Eq. (41)].

Case 3: Imposed Constant Discharge Velocity to Upper Boundary of a Semi-infinite Column

As in Cases 1 and 2, the initial condition for this case is described by a uniform initial moisture content, as expressed by Eq. (29). In contrast, a Neumann flux boundary condition is adopted for the upper boundary. This involves imposing a constant discharge velocity to the upper boundary of the domain as follows

$$\left(\bar{D}_z\frac{\partial \theta}{\partial z} - k_z\right)\Big|_{z=0} = v_0 \tag{50}$$

where v_0 = constant. The maximum discharge velocity that can be physically imposed corresponds to the soil saturated hydraulic conductivity (k_s). Specifically, the maximum imposed discharge velocity is

$$v_{0,\max} = \frac{\theta_s k_s}{(\theta_s - \theta_r)} \tag{51}$$

As in Case 1, the lower boundary condition for the semi-infinite column in Case 3 is described by Eq. (31). Solutions to partial differential equations with these types of initial and boundary conditions have been reported for contaminant transport problems (Mason and Weaver 1924; Lindstrom et al. 1967; Gershon and Nir 1969).

The analytical solution of Eq. (26) for these initial and boundary conditions was obtained as follows:

$$\theta(z,t) = \theta_i + \left[\frac{v_0}{k_s}(\theta_s - \theta_r) - \theta_i\right]C(z,t) \tag{52}$$

where

$$C(z,t) = \frac{1}{2}\text{erfc}(Z_{-1}) + \sqrt{\frac{\bar{a}_s^2 t}{\pi \bar{D}_z}}\exp\left[-\frac{(z-\bar{a}_s t)^2}{4\bar{D}_z t}\right]$$

$$-\frac{1}{2}\left(-1 + \frac{\bar{a}_s z}{\bar{D}_z} + \frac{\bar{a}_s^2 t}{\bar{D}_z}\right)\exp\left(\frac{\bar{a}_s z}{\bar{D}_z}\right)\text{erfc}(Z_{+1}) \quad (53)$$

In the particular case where $\bar{a}_s = 0$, the analytical solution of Eq. (26) for these initial and boundary conditions reduces to

$$\theta(z,t) = \theta_i + \left[\frac{v_0}{k_s}(\theta_s - \theta_r) - \theta_i\right]\text{erfc}\left(\frac{z}{2\sqrt{\bar{D}_z t}}\right) \quad (54)$$

Also, in the particular case where $\bar{D}_z = 0$, the analytical solution of Eq. (26) for these initial and boundary conditions reduces to

$$\theta(z,t) = \theta_i + \left[\frac{v_0}{k_s}(\theta_s - \theta_r) - \theta_i\right]H(\bar{a}_s t - z) \quad (55)$$

where H = Heaviside function given by Eq. (38).

The steady-state solution can also be obtained for this case by solving Eq. (27). Specifically, the Neumann flux boundary condition is adopted in this case, which involves a constant discharge velocity imposed to the upper boundary of the domain

$$\left(\bar{D}_z\frac{d\theta}{dz} - k_z\right)\Big|_{z=0} = v_0 \quad (56)$$

where v_0 = constant. The lower boundary condition for the semi-infinite column is described by Eq. (40), as in Case 1.

The analytical solution for steady-state conditions using these boundary conditions reduces to

$$\theta(z) = \frac{v_0}{k_s}(\theta_s - \theta_r) \quad (57)$$

Case 4: Imposed Constant Discharge Velocity to Upper Boundary of a Column of Finite Length

As in Cases 1–3, the initial condition for this case is described by a uniform initial moisture content, as expressed by Eq. (29). As in Case 3, the Neumann flux boundary condition is adopted for the upper boundary, which involves imposing a constant discharge velocity [Eq. (50)].

Also as in Case 3, the maximum discharge velocity that can be imposed is defined by Eq. (51). For a column of length L, the adopted lower boundary condition corresponds to a zero gradient of the volumetric water content, which is expressed by Eq. (42). Solutions to partial differential equations with these types of initial and boundary conditions have been reported for contaminant transport problems (Bastian and Lapidus 1956; Brenner 1962).

The analytical solution of Eq. (26) for these initial and boundary conditions was deduced as follows:

$$\theta(z,t) = \theta_i + \left[\frac{v_0}{k_s}(\theta_s - \theta_r) - \theta_i\right]D(z,t) \quad (58)$$

where

$$D(z,t) = 1 - \sum_{m=1}^{\infty}\frac{\frac{2\bar{a}_s L}{\bar{D}_z}\beta_m\left[\beta_m\cos\left(\frac{\beta_m z}{L}\right) + \frac{\bar{a}_s L}{2\bar{D}_z}\sin\left(\frac{\beta_m z}{L}\right)\right]\exp\left(\frac{\bar{a}_s z}{2\bar{D}_z} - \frac{\bar{a}_s^2 t}{4\bar{D}_z} - \frac{\beta_m^2 \bar{D}_z t}{L^2}\right)}{\left[\beta_m^2 + \frac{\bar{a}_s L}{\bar{D}_z} + \left(\frac{\bar{a}_s L}{2\bar{D}_z}\right)^2\right]\left[\beta_m^2 + \left(\frac{\bar{a}_s L}{2\bar{D}_z}\right)^2\right]} \quad (59)$$

where β_m = eigenvalues corresponding to the positive roots of the equation

$$\beta_m\cot(\beta_m) - \frac{\beta_m^2\bar{D}_z}{\bar{a}_s L} + \frac{\bar{a}_s L}{4\bar{D}_z} = 0 \quad (60)$$

It is only necessary to consider approximately four terms of the series in Eq. (59) to reach accurate results. In this case, Eq. (59) can be approximated by

$$D(z,t) = \frac{1}{2}\text{erfc}(Z_{-1}) + \sqrt{\frac{\bar{a}_s^2 t}{\pi\bar{D}_z}}\exp\left[-\frac{(z-\bar{a}_s t)^2}{4\bar{D}_z t}\right]$$

$$-\frac{1}{2}\left(-1 + \frac{\bar{a}_s x}{\bar{D}_z} + \frac{\bar{a}_s^2 t}{\bar{D}_z}\right)\exp\left(\frac{\bar{a}_s z}{\bar{D}_z}\right)\text{erfc}(Z_{+1})$$

$$+\sqrt{4\frac{\bar{a}_s^2 t}{\pi\bar{D}_z}}\left[1 + \frac{\bar{a}_s}{4\bar{D}_z}(2L - z + \bar{a}_s t)\right]$$

$$\times\exp\left[\frac{\bar{a}_s L}{\bar{D}_z} - \frac{1}{4\bar{D}_z t}(2L - z + \bar{a}_s t)^2\right]$$

$$-\frac{\bar{a}_s}{\bar{D}_z}\left[2L - z + \frac{3\bar{a}_s t}{2} + \frac{\bar{a}_s}{4\bar{D}_z}(2L - z + \bar{a}_s t)^2\right]$$

$$\times\exp\left(-\frac{\bar{a}_s L}{\bar{D}_z}\right)\text{erfc}\left(\frac{2L - z + \bar{a}_s t}{2\sqrt{\bar{D}_z t}}\right) \quad (61)$$

In the particular case where $\bar{a}_s = 0$, the approximated solution of Eq. (26) for these initial and boundary conditions reduces to Eq. (54), which is the same solution obtained for Case 3. Also, in the particular case where $\bar{D}_z = 0$, the analytical solution of Eq. (26) for these initial and boundary conditions reduces to Eq. (55).

A steady-state solution can also be obtained for this case. Specifically, as in Case 3, the Neumann flux boundary condition is adopted, which involves a constant discharge velocity imposed to the upper boundary of the domain [Eq. (56)]. As in Case 2, for a column of length L, a lower boundary condition corresponding to zero

gradient in the volumetric water content is imposed at the lower end of the domain, as expressed by Eq. (49). The analytical solution for steady-state conditions using these boundary conditions is the same as that obtained for Case 3, and reduces to that defined by Eq. (57).

Parametric Evaluations

The availability of analytical solutions for complex transient problems, such as unsaturated flow in porous media, is particularly beneficial to assess the sensitivity of the variables that govern the flow process. Accordingly, this section provides an evaluation of the sensitivity of key parameters using the analytical solutions of Richard's equation developed in this study. Parametric evaluations were conducted considering both semi-infinity columns (Cases 1 and 3) and columns with a finite length (Cases 2 and 4). The values adopted in these evaluations for parameters θ_r, θ_s, and k_s are 0.04, 0.41, and 8.2×10^{-7} m/s, respectively. Different values of the hydraulic parameter δ were used ($\delta = 0.003$, 0.03, and 0.3 kPa^{-1}) to assess the effect of the shape of the hydraulic functions. The initial and boundary conditions adopted in the parametric evaluations for Cases 1 and 2 correspond to $\theta_i = 0.13$ and $\theta_0 = 0.26$, respectively. For Cases 3 and 4, the adopted initial and boundary conditions correspond to $\theta_i = 0.13$ and $v_0 = 5.7 \times 10^{-7}$ m/s, respectively.

Fig. 5 shows a set of results for the analytic solution, presented as the time history of volumetric water content at a given depth (z) for Case 1 ($\delta = 0.03\ \text{kPa}^{-1}$ for $z = 0.06$ m). Three distinct periods can be observed in the time history. Specifically, Period 1 represents the time (ending at approximately $t = 200$ min in the figure) during which the moisture remains at its initial volumetric water content ($\theta_i = 0.13$). Period 2 corresponds to a transition period during which the volumetric water content rises gradually from θ_i to θ_0. Finally, Period 3 represents conditions approaching steady state (starting at approximately $t = 1{,}000$ min in the figure), after which the moisture has reached the volumetric water content imposed on the upper boundary of the domain ($\theta_0 = 0.26$). The maximum moisture change rate $[(\partial\theta/\partial t)_{\max}]$ is also shown in Fig. 5, and occurs at a moisture content (θ_{ave}) that corresponds to the average value between θ_0 and θ_i.

Fig. 6 shows the time history of volumetric water content for Case 1 when $\delta = 0.03\ \text{kPa}^{-1}$ for different locations (z). Fig. 6(a) corresponds to the solution for the case in which both advective and diffusive flow components are relevant [Eq. (33)], whereas Fig. 6(b) corresponds to a problem dominated by advective flow [Eq. (37)], and Fig. 6(c) corresponds to a problem dominated by diffusive flow [Eq. (36)].

The results in Fig. 6(a) illustrate that the maximum rate of moisture change $[(\partial\theta/\partial t)_{\max}]$ decreases with increasing values of z. That is, the moisture front spreads with increasing travel distance because of the diffusive component of the unsaturated flow. In contrast, as can be seen in Fig. 6(b), there is no spreading of the

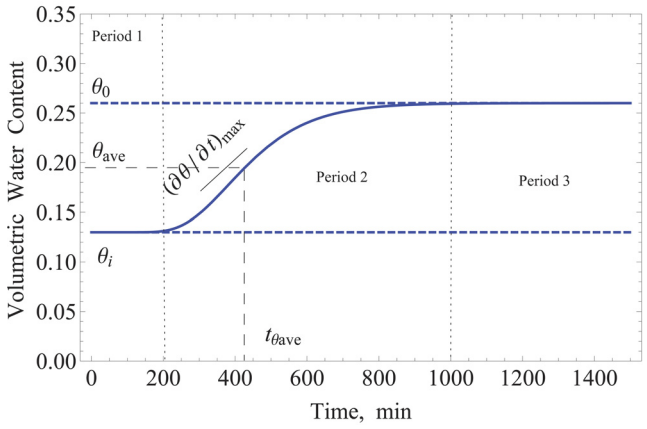

Fig. 5. (Color) Distinct periods in predicted time history of volumetric water content for Case 1 ($\delta = 0.03\ \text{kPa}^{-1}$, $z = 0.06$ m) considering advective and diffusive flow components [Eq. (33)]

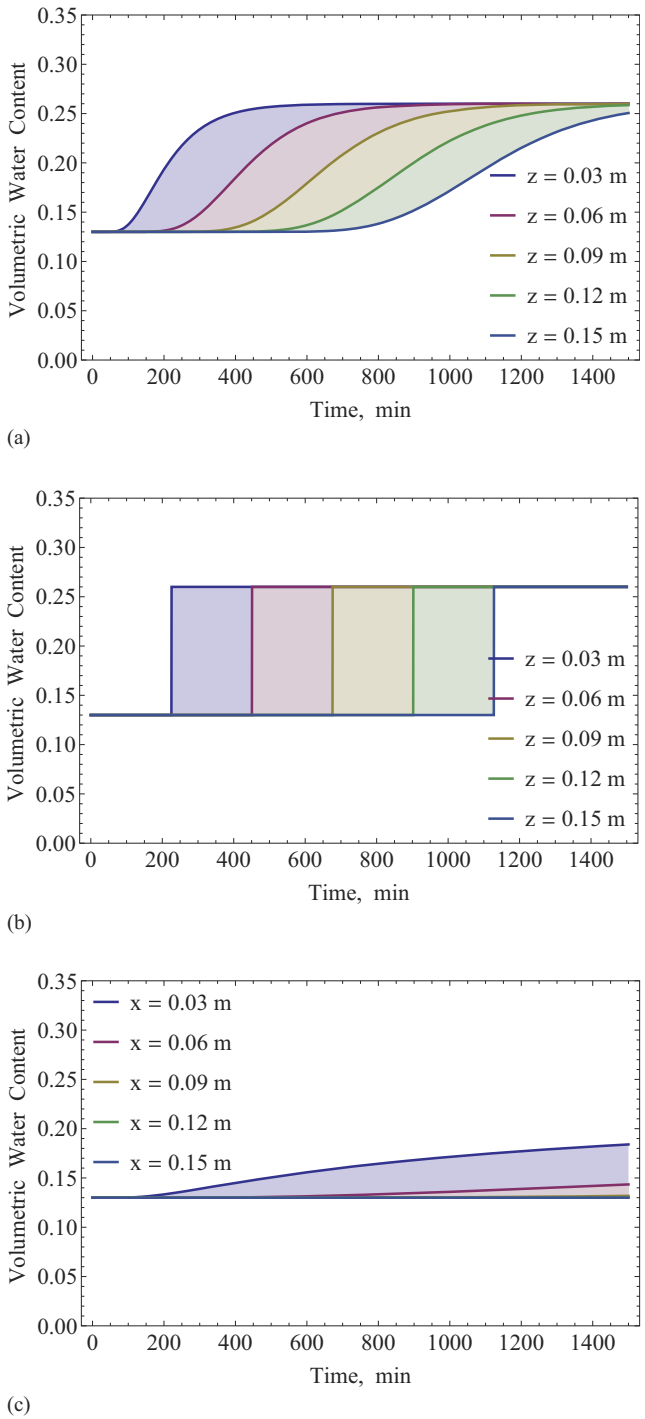

Fig. 6. (Color) Predicted time history of volumetric water content for Case 1 at different locations ($\delta = 0.03\ \text{kPa}^{-1}$) considering (a) both advective and diffusive flow components [Eq. (33)]; (b) only advective flow [Eq. (37)]; and (c) only diffusive flow [Eq. (36)]

moisture front when flow is dominated by the advective component. In this case, as the moisture front advances, the moisture changes suddenly from its initial value ($\theta_i = 0.13$) to the volumetric water content imposed on the upper boundary ($\theta_0 = 0.26$). Finally, Fig. 6(c) illustrates the results of a problem dominated by diffusive flow. It corresponds, for example, to one-dimensional unsaturated flow advancing in the horizontal, x-direction (i.e., in a direction where there is no gravity-induced flow). As can be observed in this figure, the time required for the moisture to start increasing beyond the initial volumetric water content ($\theta_i = 0.13$) increases with increasing x. Also, the steady-state condition is far from being reached for the time scale shown in the figure.

Fig. 7 shows the the time history for a case in which both advective and diffusive flow components are relevant, superimposed with the time history for a case in which only advective flow is relevant (for Case 1, $\delta = 0.03\,\text{kPa}^{-1}$). The results in Fig. 7 indicate that the time ($t_{\theta\text{ave}}$) to reach θ_{ave} (at a given location z) in a problem with both advective and diffusive flow components is somewhat shorter than the time (t_a) to reach θ_{ave} in a problem dominated by advective flow.

The availability of the analytical solutions obtained in this study allows defining parameters to better understand the flow process. Specifically, $v_{\theta\text{ave}}$ and v_a are defined as the velocities corresponding to θ_{ave} in problems where both advective and diffusive flow components are relevant and where advective flow dominates, respectively. They correspond to velocities computed as $z/t_{\theta\text{ave}}$ and z/t_a, respectively. Fig. 8(a) shows the values obtained for $v_{\theta\text{ave}}$ and v_a in the problem being evaluated. As shown in the figure, v_a remains constant and equals $\bar{a}_s$ (the constant unsaturated advective seepage). In contrast, $v_{\theta\text{ave}}$ is always higher than v_a and decreases with increasing z. Fig. 8(b) presents the ratio $v_{\theta\text{ave}}/v_a$, which shows a decreasing trend with increasing z, and tends to 1 for high z values.

Fig. 9 shows a typical profile of moisture content at a given time (t). Three distinct zones can be observed in this particular moisture profile obtained for Case 1 ($t = 300\,\text{min}$, $\delta = 0.03\,\text{kPa}^{-1}$). Specifically, Zone 1 corresponds to the region where the moisture has already reached the volumetric water content imposed on the upper boundary of the domain ($\theta_0 = 0.26$). Zone 2 is a transient zone where the volumetric water content gradually decreases from θ_0 to θ_i. Finally, Zone 3 corresponds to the region where the moisture still remains at its initial value ($\theta_i = 0.13$).

Fig. 10 shows the predicted moisture profiles at different times for Case 1 (considering $\delta = 0.03\,\text{kPa}^{-1}$). Fig. 10(a) corresponds to the case in which both advective and diffusive flow components are relevant, whereas Fig. 10(b) corresponds to a problem dominated by advective flow, and Fig. 10(c) corresponds to a problem dominated by diffusive flow.

Inspection of Fig. 10(a) reveals that $(\partial\theta/\partial z)_{\text{max}}$ decreases with increasing time. That is, spreading of the moisture front increases with time because of the diffusion component of the unsaturated flow. In contrast, the results in Fig. 10(b) show that there is no spreading of the moisture front when advection dominates the flow. In this case, as the moisture front advances, the moisture changes

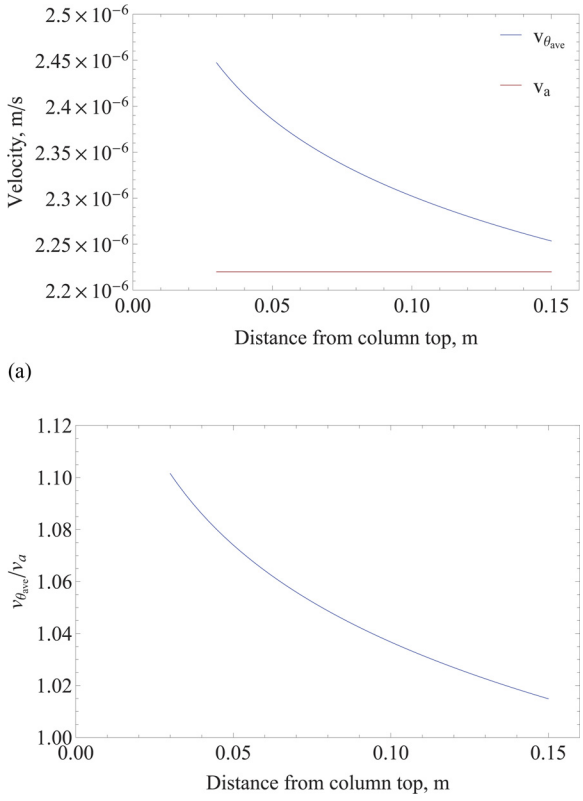

Fig. 8. (Color) Velocity at the column: (a) $v_{\theta\text{ave}}$ and v_a; (b) ratio $v_{\theta\text{ave}}/v_a$

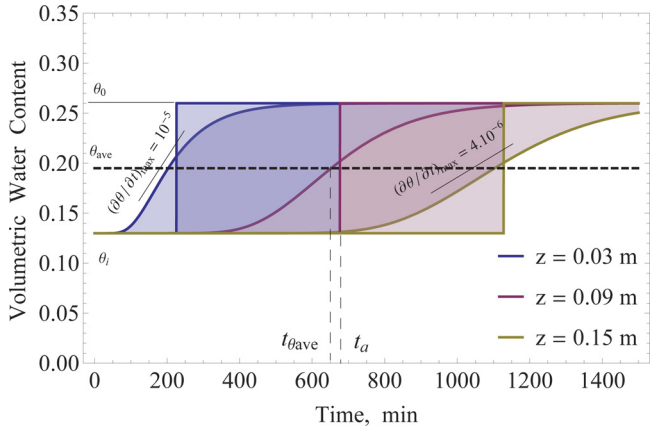

Fig. 7. (Color) Comparison between time histories of volumetric water content in a problem involving multiple flow components and in a problem with only advective flow (Case 1, $\delta = 0.03\,\text{kPa}^{-1}$)

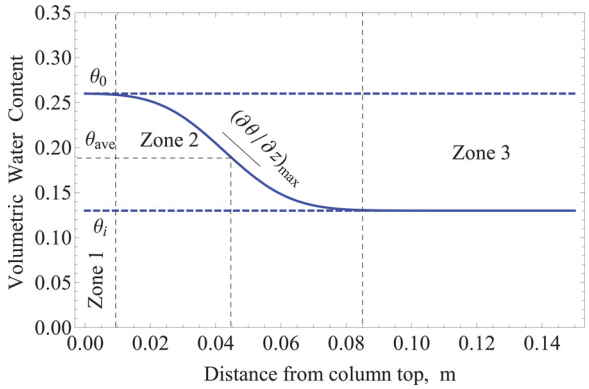

Fig. 9. (Color) Distinct zones for predicted moisture profile for Case 1 ($\delta = 0.03\,\text{kPa}^{-1}$, $t = 300\,\text{min}$) considering advective and diffusive components [Eq. (33)]

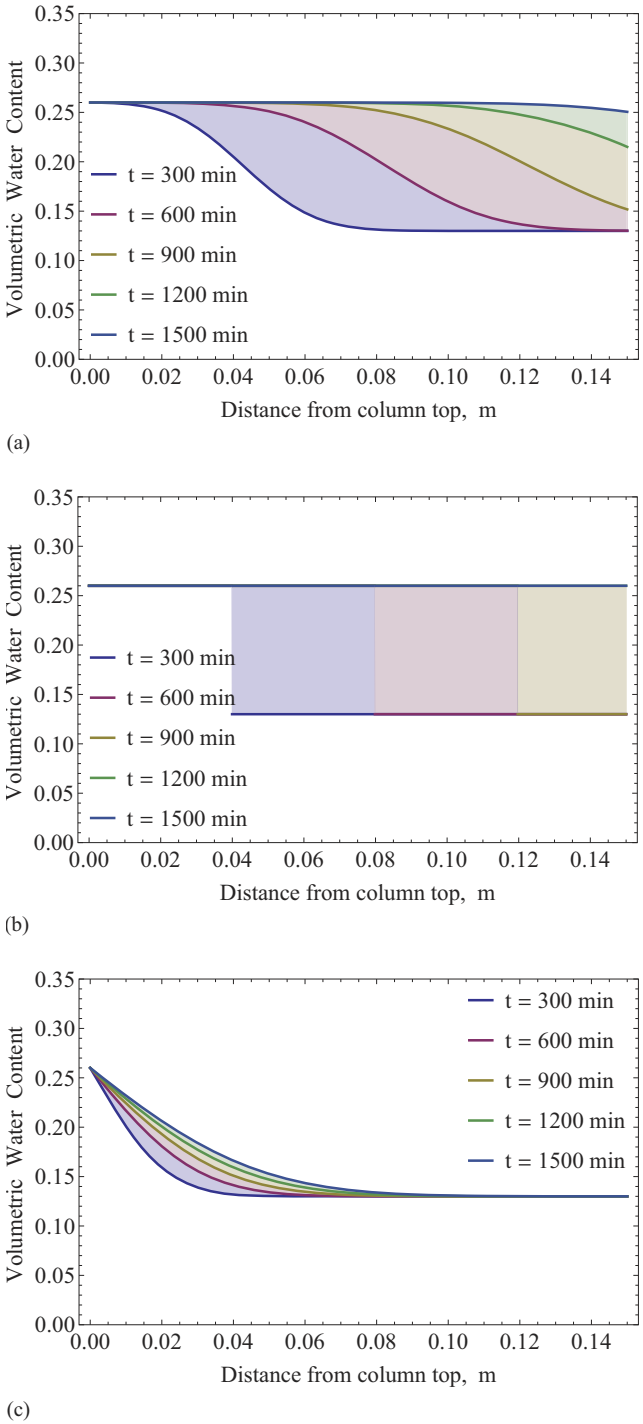

Fig. 10. (Color) Predicted moisture profiles for Case 1 at increasing time ($\delta = 0.03\,\text{kPa}^{-1}$) considering (a) both advective and diffusive flow components [Eq. (33)]; (b) only advective flow [Eq. (37)]; and (c) only diffusive flow [Eq. (36)]

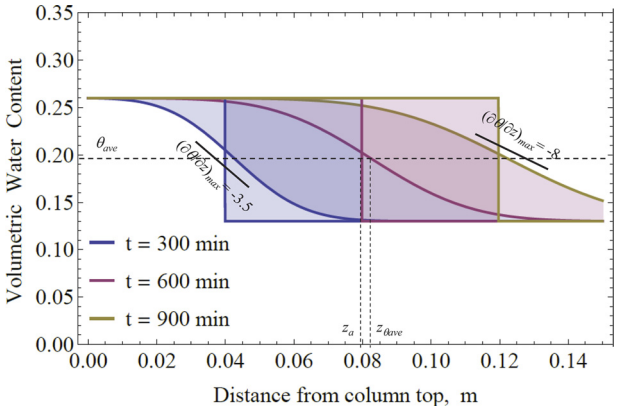

Fig. 11. (Color) Comparison between moisture profiles in a problem involving multiple flow components and in a problem with only advective flow (Case 1, $\delta = 0.03\,\text{kPa}^{-1}$)

suddenly from the volumetric water content imposed on the upper boundary ($\theta_0 = 0.26$) to the initial moisture content ($\theta_i = 0.13$). Fig. 10(c) illustrates the results of a problem dominated by diffusive flow (e.g., one-dimensional unsaturated flow in the x-direction). As can be observed in this figure, the moisture gradients decrease with increasing time.

Fig. 11 shows the moisture profiles (for Case 1, $\delta = 0.03\,\text{kPa}^{-1}$) for a case where both advective and diffusive flow components are relevant, superimposed with the moisture profiles for a case in which only advective flow is relevant. Inspection of Fig. 11 reveals that the distance ($z_{\theta\text{ave}}$) that reaches a moisture (θ_{ave}) [at a given time (t)] in a problem with both advective and diffusive flow components is somewhat larger than the distance (z_a) reached by the moisture front in a case dominated by advective flow.

Fig. 12(a) shows the time history of the rates of moisture change ($\partial\theta/\partial t$) for Case 1 ($\delta = 0.03\,\text{kPa}^{-1}$) for a problem with both advective and diffusive flow components [Eq. (33)]. In addition, Fig. 12(b) shows these rates for a problem dominated by advection [Eq. (37)], whereas Fig. 12(c) shows these rates for a problem dominated by diffusion [Eq. (36)].

The results in Fig. 12(a) illustrate that, for a given location (z), the rate of moisture change is zero for an initial period during which the moisture remains at its initial value (Period 1 in Fig. 5). The rate of moisture change then increases, reaching a peak value [$(\partial\theta/\partial t)_{\max}$] at time $t_{\theta\text{ave}}$. This peak value corresponds to the maximum slope observed in Fig. 5. Beyond the time corresponding to the peak rate, the rate of moisture change decreases to zero. Beyond this time (Period 3 in Fig. 5), the moisture has reached the volumetric water content imposed on the upper boundary of the domain ($\theta_0 = 0.26$). The results in Fig. 12(a) also show that the peak rate of moisture change decreases with increasing time. In addition, the width between the initial and final tails of each curve can be observed to increase with increasing distance (z) from the upper boundary. It can be demonstrated that the total area (integral of $\partial\theta/\partial t$ from 0 to $+\infty$) under each of the moisture rate curves is the same for the different values of z. The decreasing peak and increasing width of the moisture rate curves, for increasing z values, are trends that depend on the diffusive component of the unsaturated flow.

As can be seen in Fig. 12(b), when flow is dominated by an advective component, the moisture rate function shows an infinity peak value ($\partial\theta/\partial t_{\max} = +\infty$), which occurs at the time (t_a) that corresponds to the arrival of the moisture front. At this time, the volumetric moisture content increases suddenly from its initial value to the value imposed at the upper boundary of the domain ($\theta_0 = 0.26$).

Fig. 12(c) shows the moisture rate curves of a problem dominated by diffusive flow. The trends observed with increasing x values are similar to those observed in Fig. 12(a) for a case involving both advective and diffusive flow components. However, it should be noted that the magnitudes of the rates (e.g., the peak values) are significantly smaller than those obtained when advective flow is also present.

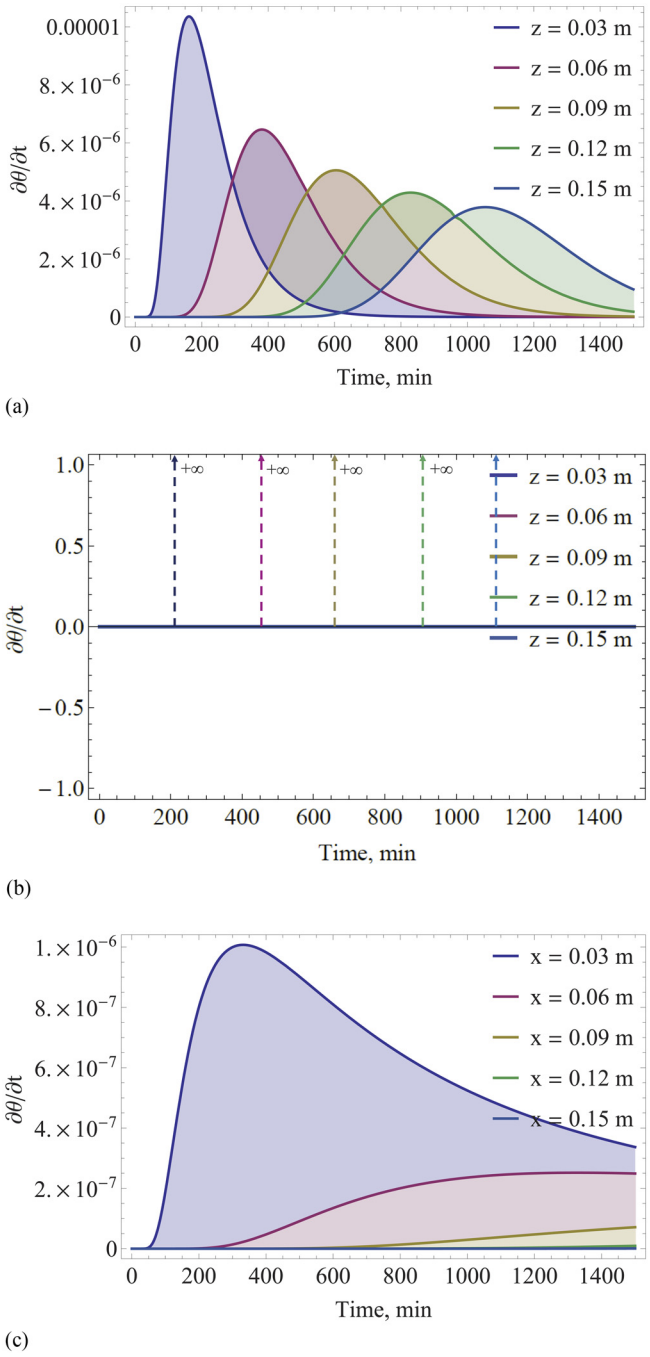

Fig. 12. (Color) Predicted time history of rates in moisture change for Case 1 at different locations ($\delta = 0.03\,\text{kPa}^{-1}$) considering (a) both advective and diffusive components [Eq. (33)]; (b) only advective flow [Eq. (37)]; and (c) only diffusive flow [Eq. (36)]

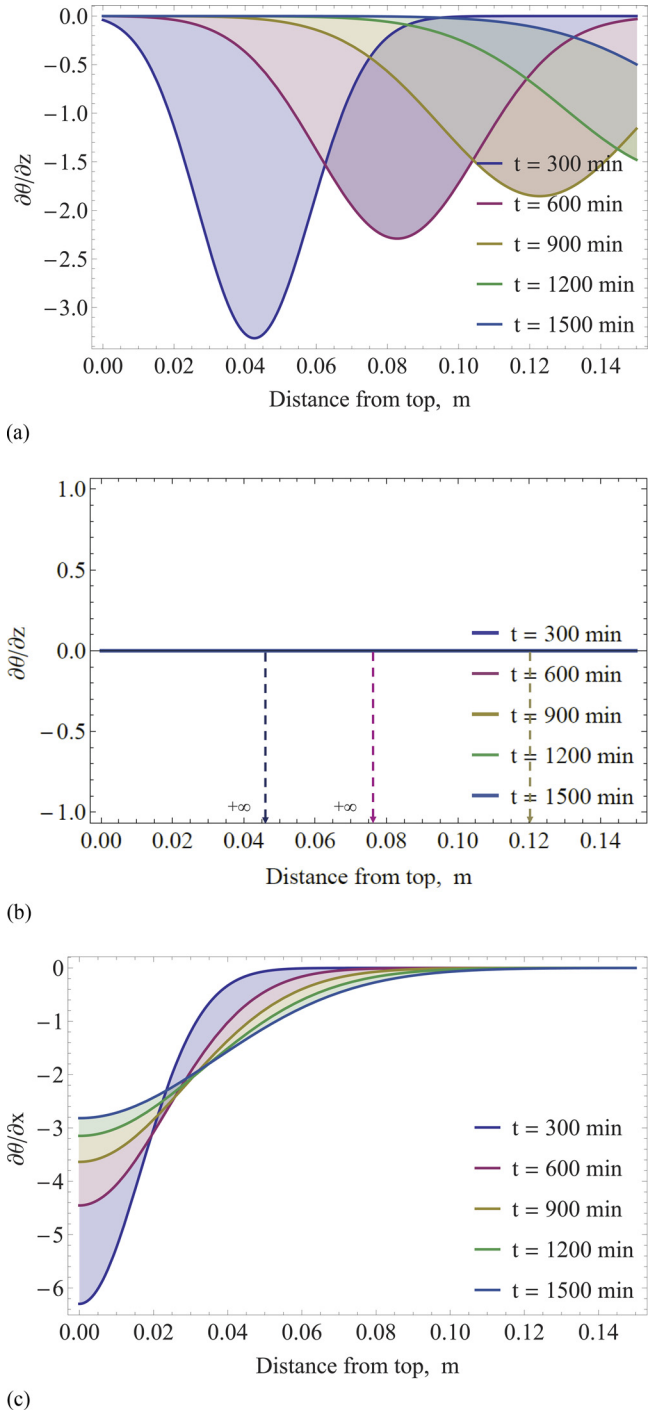

Fig. 13. (Color) Predicted profiles of moisture gradients for Case 1 at increasing time ($\delta = 0.03\,\text{kPa}^{-1}$) considering (a) both advective and diffusive flow components [Eq. (33)]; (b) only advective flow [Eq. (37)]; and (c) only diffusive flow [Eq. (36)]

Fig. 13(a) shows the profiles of moisture content gradients ($\partial\theta/\partial z$) for Case 1 ($\delta = 0.03\,\text{kPa}^{-1}$) for a problem where both advective and diffusive flow components are relevant [Eq. (33)]. Also, Fig 13(b) shows these gradients for a problem with only advective flow [Eq. (37)], whereas Fig. 13(c) shows such gradients for a problem with only diffusive flow [Eq. (36)].

The results in Fig. 13(a) illustrate that, for a given time (t), the moisture gradients remain at zero for an initial period (Zone 1 in Fig. 9). They subsequently increase (in absolute value), reaching a peak value [$(\partial\theta/\partial z)_{\max}$] at time $t_{\theta\text{ave}}$. This peak value corresponds to the maximum slope observed in Fig. 9. Beyond this location, the moisture gradients decrease until reaching zero, which corresponds to the beginning of Zone 3. The results in Fig. 13(a) also show that the value of the peak moisture gradients decreases (in absolute value) with increasing time. It can also be observed that the width between the initial and final tails of each moisture gradient curve increases with increasing time. It can be demonstrated that the total area (integral of $\partial\theta/\partial z$ from 0 to $+\infty$) under each of the moisture gradient curves is the same for different values of t. The decreasing

peak (in absolute value) and increasing width of the moisture gradient curves, for increasing time, are trends that depend on the diffusive component of the unsaturated flow.

As can be seen in Fig. 13(b), the moisture gradient shows an infinity peak value ($\partial\theta/\partial z_{max} = -\infty$) when flow is dominated by an advective component, with the peak occurring at distance z_a corresponding to the arrival of the moisture front. At this location, the moisture content increases suddenly from its initial value to the value imposed at the upper boundary of the domain ($\theta_0 = 0.26$).

Fig. 13(c) shows the moisture gradient curves of a problem dominated by diffusive flow. The trends observed with increasing time are consistent with those observed in Fig. 13(a) for a case involving both advective and diffusive flow components. However, the magnitude of the gradients (e.g., the peak values) are significantly higher (in absolute values) than those obtained when advective flow is also present.

Fig. 14 illustrates the time histories of the advective flow [Eq. (20)] and the dispersive flow [Eq. (21)], respectively, for Case 1 ($\delta = 0.03\,\text{kPa}^{-1}$). Fig. 14(a) illustrates that the advective flow increases with increasing time until reaching a peak value. Comparison of Figs. 14(a) and 6(a) reveals that the maximum advective flow is reached at the time when the steady-state condition has been reached. Beyond this time, the volumetric water content will remain at the value imposed on the upper boundary of the domain ($\theta_0 = 0.26$), with the advective flow component remaining constant. Fig. 14(b) also shows that the diffusive flow increases with increasing time until reaching a peak value, beyond which the diffusive flow component decreases. The maximum diffusive flow is reached at the same time as the peak rate in moisture changes [Fig. 12(a)]. As can be seen in Fig. 14(b), the diffusive flow ultimately decreases to zero. Accordingly, the unsaturated flow is ultimately controlled by the advective flow component [Fig. 14(a)].

It should be noted that the magnitude of the peak value of the advective flow component [Fig. 14(a)] is over an order of magnitude higher than the peak value of the diffusive flow component [Fig. 14(b)] for the parameters adopted in this example. Accordingly, whereas the diffusive flow is not negligible, the advective flow was found to be the most relevant component for the unsaturated flow problem illustrated in this example.

Fig. 15 shows the advective and the difussive flow profiles with increasing time for Case 1 ($\delta = 0.03\,\text{kPa}^{-1}$). Fig. 15(a) shows that the advective flow decreases with increasing distance until reaching zero. Fig. 15(b) shows that the diffusive flow initially increases with increasing distance until reaching a peak value, beyond which the diffusive flow decreases. The location of the peak diffusive flow corresponds to the location of the peak moisture gradients [Fig. 13(a)]. As shown in Fig. 15(b), the diffusive flow ultimately tends to zero at high values of z.

To assess the effect of the hydraulic parameter (δ), Fig. 16 shows the results obtained for Case 1, but considering $\delta = 0.3\,\text{kPa}^{-1}$ instead of $0.03\,\text{kPa}^{-1}$. Consistent with previous discussions, increasing values of δ led to a decreasing air-entry pressure (Fig. 2), an increasing $(\partial\theta/\partial\psi)_{initial}$ (Fig. 3), and an increasing $(\partial k/\partial\psi)_{initial}$ (Fig. 4).

Comparison of the results shown in Figs. 16(a and b) with the results shown in Figs. 6(a) and 13(a) reveals that increasing values of the parameter δ leads to increasing rates of moisture change and, in particular, to increasing values of $(\partial\theta/\partial t)_{max}$. Accordingly, the volumetric water content (θ_0) imposed on the upper boundary of

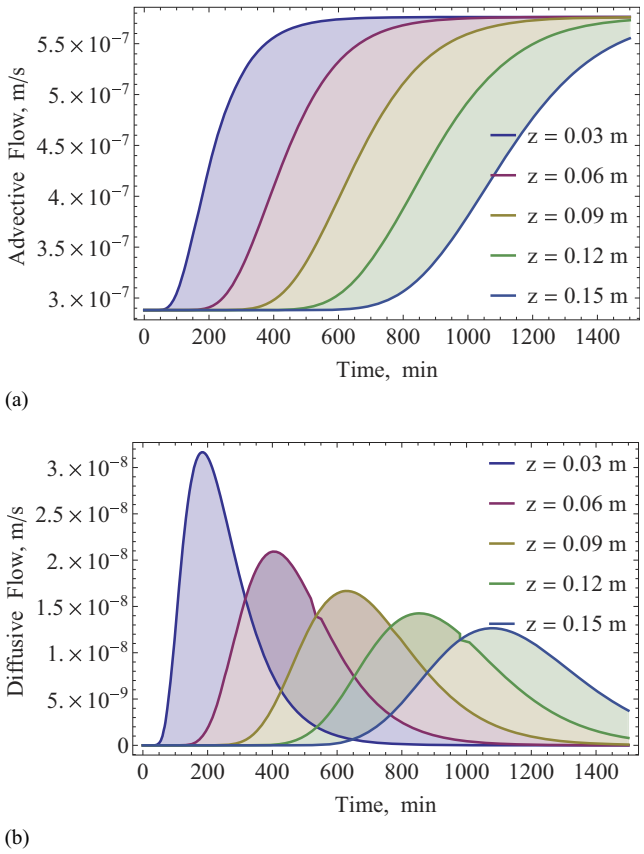

Fig. 14. (Color) Predicted profiles of (a) advective flow and (b) diffusive flow at increasing times for Case 1 (when $\delta = 0.03\,\text{kPa}^{-1}$)

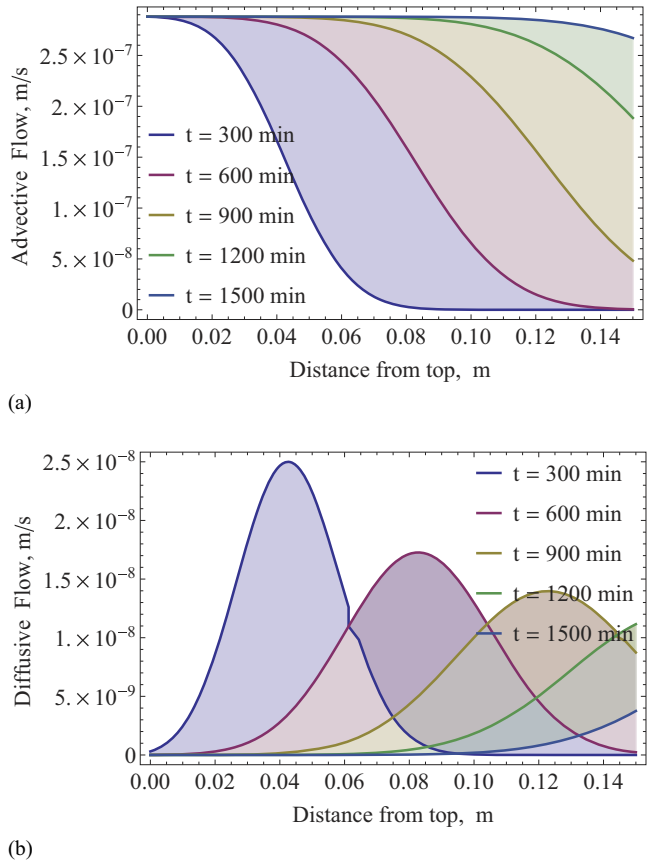

Fig. 15. (Color) Predicted profiles of (a) advective flow and (b) diffusive flow at different locations for Case 1 (when $\delta = 0.03\,\text{kPa}^{-1}$)

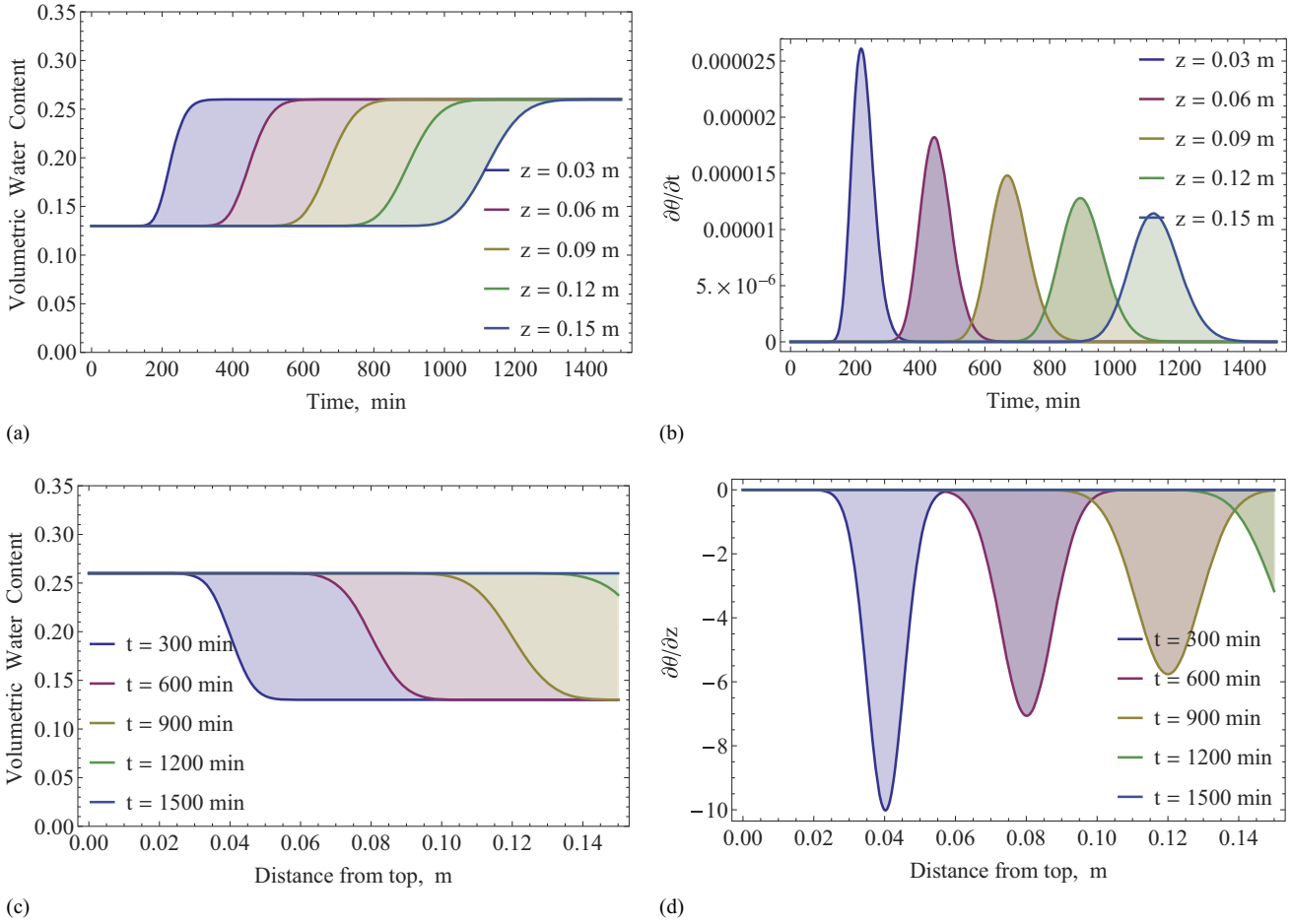

Fig. 16. (Color) Predicted results for Case 1 using $\delta = 0.3\,\text{kPa}^{-1}$: (a) time history of moisture content; (b) time history of moisture rates; (c) moisture profiles; (d) moisture gradient profiles

the domain is reached earlier, at a given location (z), for increasing values of δ.

Comparison of the results shown in Figs. 16(c and d) with the results shown in Figs. 10(a) and 13(a) reveals that increasing values of the parameter δ lead to increasing (in absolute value) gradients of moisture change and, in particular, to increasing values of $(\partial\theta/\partial z)_{\max}$. Accordingly, the imposed volumetric moisture (θ_0) is reached earlier for higher values of δ.

In addition to evaluating the results for Case 1 (semi-infinite column), the type of results presented in Figs. 5–16 were also obtained after conducting analyses using the boundary conditions corresponding to Case 2 (column of finite length). It was observed that differences in the results obtained between these two cases, as shown by their time histories and moisture profiles, were negligible. Accordingly, the analytical solution for Case 1, which is comparatively simpler than that for Case 2, could be used to preliminarily solve problems involving columns of finite length.

Fig. 17 shows the results obtained when using the boundary conditions corresponding to Case 3. Specifically, a constant discharge velocity ($v_0 = 5.7 \times 10^{-7}$ m/s) was imposed to the upper boundary of a semi-infinite column.

Consistent with the results obtained for Cases 1 and 2, the results in Fig. 17(a) show that the rate $(\partial\theta/\partial t)_{\max}$ decreases with increasing values of z. Also consistent with the results obtained for Cases 1 and 2, the results in Fig. 17(b) show that the gradient $(\partial\theta/\partial z)_{\max}$ decreases with increasing time. Both responses can be attributed to the spreading effect of the moisture front related to the diffusive component of the unsaturated flow.

Fig. 18 shows the effect of varying the constant discharge velocity imposed on the upper boundary of a semi-infinity column. The curves correspond to the predicted time history of volumetric water content for Case 3 ($\delta = 0.03\,\text{kPa}^{-1}$) at a given location ($z = 0.06$ m) for three different values of the imposed constant discharge velocity ($v_0 = 4.5 \times 10^{-7}$, 5.0×10^{-7}, and 5.7×10^{-7} m/s). As shown in the figure, increasing values of the imposed discharge velocity lead to increasing values of volumetric water content. In particular, the moisture content reached after a comparatively long time will tend to a constant value (θ_∞), which is directly proportional to v_0, as follows:

$$\theta_\infty = \frac{v_0}{k_s}(\theta_s - \theta_r) \tag{62}$$

It should be noted that the value of θ_∞ in Eq. (62) is the same as the value obtained for the steady-state solution previously obtained for Case 3 [Eq. (57)]. Indeed, the value of $v_0 = 5.7 \times 10^{-7}$ m/s adopted for the analyses presented in Fig. 17 corresponds to an imposed flow that would lead to $\theta_\infty = 0.26$ (i.e., the value of imposed moisture adopted previously for Cases 1 and 2).

In addition to evaluating the results for Case 3 (semi-infinite column), the analyses presented in Figs. 17 and 18 were also conducted using the boundary conditions corresponding to Case 4 (column of finite length). It was observed that differences in the results obtained

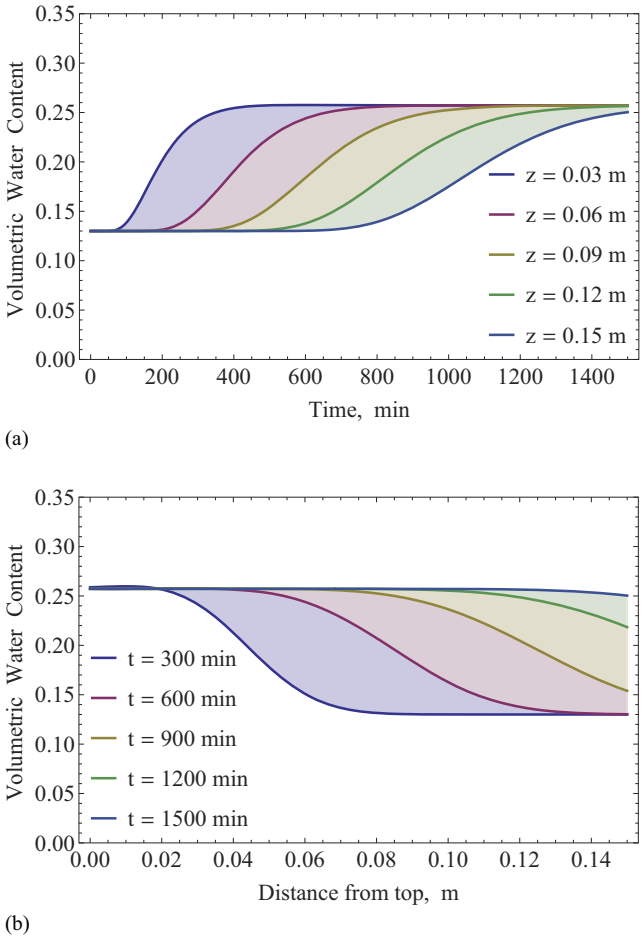

Fig. 17. (Color) Predicted volumetric water content for Case 3 (δ = 0.03 kPa^{-1}): (a) time history at different locations; (b) profiles at increasing times

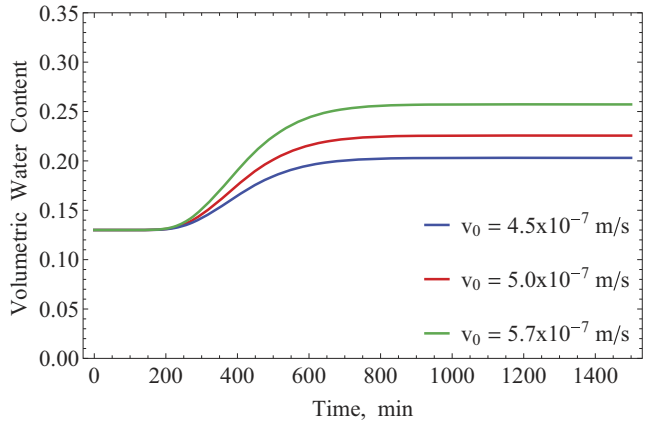

Fig. 18. (Color) Effect of varying imposed constant discharge velocity in the upper boundary of a semi-infinite column

in these two cases, as shown by their time histories and moisture profiles, were negligible. Accordingly, the analytical solution for Case 3, which is comparatively simpler than that for Case 4, could be used to preliminarily solve problems involving columns of finite length.

Conclusions

This paper presents a series of analytical solutions of Richard's equation for unsaturated flow under transient conditions. The solutions were developed for a variety of initial and boundary conditions, including an imposed moisture content and an imposed discharge velocity value on the boundary, as well as considering an infinitely long column or a column of finite length. The obtained closed-form solutions to Richard's equation are particularly valuable to (1) facilitate parametric evaluations, and (2) validate the accuracy of numerical predictions. This paper presents the development of the analytical solutions and associated parametric evaluations. The development of efficient numerical schemes as well as comparisons between analytical results and numerical predictions are presented in a companion paper (Cavalcante and Zornberg 2017). The solution of Richard's equation is illustrated in the paper using representative examples that consider a variety of boundary conditions. The analytical solutions allowed representation of (1) the time history of volumetric water content at different locations, and (2) the moisture profiles at different times.

Based on the results obtained from this study, the following general conclusions can be drawn:

- The use of the volumetric water content as a dependent variable in Richard's equation allowed rewriting this equation in a form that is analogous to the advection-dispersion contaminant transport equation.
- The use of a logarithmic model to represent the SWRC and of a linear model to represent the k-function, using a single hydraulic parameter (δ), was found to lead to a representation of Richard's equation in which the unsaturated water diffusivity and the unsaturated advection seepage, in the z-direction, are constants.
- Representation of Richard's equation in terms of advective and dispersive components, as well as the selection of hydraulic functions represented using the hydraulic parameter (δ) were found to lead to analytical solutions of the transient, unsaturated flow problem. The solutions were obtained using Laplace transformations in the time domain.
- The advective-diffusive representation of Richard's equation also allowed determination of analytical solutions for the particular cases in which the unsaturated flow is dominated by either the advective or the diffusive flow components. These solutions were found to provide good insight into unsaturated flow mechanisms.

In addition, the following conclusions can be drawn from a parametric evaluation as obtained considering hydraulic functions that are represented using the hydraulic parameter (δ):

- The time history of volumetric water content at a given location was found to involve three distinctive regions: (1) Period 1 when the moisture remains at its initial value; (2) Period 2 when the volumetric water content rises gradually from θ_i to θ_0; and (3) Period 3, corresponding to the steady-state condition, when the moisture has reached its ultimate value (e.g., the volumetric water content imposed at the top boundary of the domain).
- The maximum rate of moisture changes [$(\partial\theta/\partial t)_{max}$] was found to decrease with increasing values of z. This trend can be attributed to the diffusive component of the unsaturated flow.
- The time [$t_{\theta ave}$] to reach θ_{ave} (average moisture content between the initial and steady-state final values) at a given location (z) in a problem with both advective and diffusive flow components is somewhat shorter than the time (t_a) to reach θ_{ave} in a problem dominated by advective flow.

- The velocity (v_a) corresponding to θ_{ave} in a problem with only advective flow remains constant and equals $\bar{a}_s$ (the constant unsaturated advective seepage). The velocity ($v_{\theta ave}$) corresponding to θ_{ave} in a problem with both advective and diffusive flow components was found to be higher than v_a, and to decrease with increasing z. The ratio between $v_{\theta ave}$ and v_a was found to tend to 1 for comparatively high z values.
- The moisture content profile at a given time was found to involve the following three distinctive regions: (1) Zone 1, where the moisture has already reached its steady-state value; (2) Zone 2, where the volumetric water content decreases gradually from θ_0 to θ_i; and (3) Zone 3, where the moisture stilll remains at its initial value.
- The absolute value of the maximum moisture gradient $[(\partial\theta/\partial z)_{max}]$ was found to decrease with increasing time. This trend can be attributed to the impact of the diffusive component of the unsaturated flow.
- Increasing values of the hydraulic parameter (δ) were found to correspond to increasing rates of moisture change and, in particular, to increasing $(\partial\theta/\partial t)_{max}$. Accordingly, the steady-state volumetric water content value was reached faster for higher values of δ.
- Increasing values of the hydraulic parameter (δ) were found to correspond to a decrease in the gradients (in absolute value) of moisture change and, in particular, to decreasing $(\partial\theta/\partial z)_{max}$.
- The differences between the predicted time histories and moisture profiles for Case 1 and those obtained for Case 2 were found to be minor. Accordingly, the analytical solution for Case 1, which is comparatively simpler than that for Case 2, could be used to preliminarily solve problems involving columns of finite length.
- The differences between the predicted time histories and moisture profiles for Case 3 and those obtained for Case 4 were found to be minor. Accordingly, the analytical solution for Case 3, which is comparatively simpler than that for Case 4, could be used to preliminarily solve problems involving columns of finite length.

Appendix I. Definition of Advective and Diffusive Flow Components

This appendix demonstrates that the use of advective and diffusive flow components, as defined by Eqs. (20) and (21) in the paper, leads to the conventional Richard's equation.

The continuity principle implies that the difference between the mass outflow and inflow rates should equal the rate of change in water storage (Fig. 19). That is

$$\frac{\partial\theta}{\partial t}dx\,dy\,dz = f\,dx\,dy - \left(f + \frac{\partial f}{\partial z}dz\right)dx\,dy \tag{63}$$

where f = total flow (L/T).

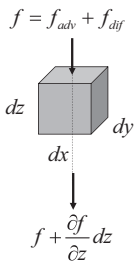

Fig. 19. Representative elementary volume

As discussed in the paper, the total flow can be grouped into two components as follows:

$$f(z,t) = f_{adv}(z,t) + f_{dif}(z,t) \tag{64}$$

where f_{adv} = advective flow component (L/T); and f_{dif} = diffusive flow component of the total flow (L/T).

The advective and the diffusive flow components, respectively, are given by

$$f_{adv}(z,t) = a_s(\theta)\theta \tag{65}$$

$$f_{dif}(z,t) = -D_z(\theta)\frac{\partial\theta}{\partial z} \tag{66}$$

Considering Eqs. (65) and (66) into Eqs. (63) and (64) leads to

$$\frac{\partial\theta}{\partial t} = -\frac{\partial}{\partial z}\left[a_s(\theta)\theta - D_z(\theta)\frac{\partial\theta}{\partial z}\right] \tag{67}$$

or

$$\frac{\partial\theta}{\partial t} = \frac{\partial}{\partial z}\left[D_z(\theta)\frac{\partial\theta}{\partial z}\right] - \frac{\partial}{\partial z}[a_s(\theta)\theta] \tag{68}$$

Using Eq. (19) in the paper, the second term on the right side of Eq. (68) can be rewritten as

$$\frac{\partial}{\partial z}[a_s(\theta)\theta] = \frac{\partial}{\partial z}\left(\frac{\partial k_z}{\partial\theta}\theta\right) = \frac{\partial k_z}{\partial\theta}\frac{\partial\theta}{\partial z} = \frac{\partial k_z}{\partial z} \tag{69}$$

Considering Eq. (69) into Eq. (68) results in Richard's equation. That is

$$\frac{\partial\theta}{\partial t} = \frac{\partial}{\partial z}\left[D_z(\theta)\frac{\partial\theta}{\partial z}\right] - \frac{\partial k_z(\theta)}{\partial z} \tag{70}$$

Eq. (70), obtained as the addition of advective and diffusive flow components, is the same as Eq. (17), obtained using the conventional discharge velocity definitions. In summary, the flow components f_{adv} and f_{dif}, as defined by Eqs. (20) and (21), combined with the continuity principle lead to Richard's equation.

Appendix II. Characteristics of Hydraulic Functions Represented Using the Hydraulic Parameter (δ)

The impact of the hydraulic parameter (δ) on relevant characteristics of the SWRC and the k-function is demonstrated in this appendix.

Characteristic 1: The initial slope of the SWRC (i.e., the slope corresponding to saturation) is directly proportional to the hydraulic parameter (δ).

Demonstration: The SWRC defined by a log-linear model [Eq. (22)] can be rewritten as

$$\theta(|\psi|) = \theta_r + (\theta_s - \theta_r)\exp(-\delta|\psi|) \tag{71}$$

The derivative of Eq. (71) in relation to ψ is

$$\frac{\partial\theta}{\partial|\psi|} = -\delta(\theta_s - \theta_r)\exp(-\delta|\psi|) \tag{72}$$

The initial slope of the SWRC can be obtained considering Eq. (72), when ψ tends to 0. That is

$$\left(\frac{\partial\theta}{\partial|\psi|}\right)_{\text{initial}} = \left(\frac{\partial\theta}{\partial|\psi|}\right)_{\psi\to 0} = -\delta(\theta_s - \theta_r) \tag{73}$$

Characteristic 2: The initial slope of the k-function curve (i.e., the slope corresponding to saturation) is directly proportional to the hydraulic parameter (δ).

Demonstration: The k-function defined by a log-linear model [Eq. (23)], can be rewritten as

$$k(|\psi|) = k_s \exp\left(-\delta|\psi|\right) \tag{74}$$

The derivative of Eq. (74) in relation to ψ is

$$\frac{\partial k}{\partial|\psi|} = -\delta k_s \exp\left(-\delta|\psi|\right) \tag{75}$$

The initial slope of the k-function can be obtained considering Eq. (75), when ψ tends to 0. That is

$$\left(\frac{\partial k}{\partial|\psi|}\right)_{\text{initial}} = \left(\frac{\partial k}{\partial|\psi|}\right)_{\psi\to 0} = \delta k_s \tag{76}$$

Acknowledgments

The authors acknowledge the support of the following agencies: the National Council for Scientific and Technological Development (CNPq) (Project 30449420127), the Coordination for the Improvement of Higher Level Personnel (CAPES) (Project 1431/14-5), the National Science Foundation (CMMI) (Grant 1335456), the University of Brasilia, and the University of Texas, Austin, for funding this research.

References

Basha, H. A. (1999). "Multidimensional linearized nonsteady infiltration with prescribed boundary conditions at the soil surface." *Water Resour. Res.*, 35(1), 75–83.

Bastian, W. C., and Lapidus, L. (1956). "Longitudinal diffusion in ion exchange and chromatographic columns. Finite column." *J. Phys. Chem.*, 60(6), 816–817.

Bear, J. (1979). *Hydraulics of groundwater*, McGraw-Hill, New York.

Biot, M. A. (1941). "General theory of three-dimensional consolidation." *J. Appl. Phys.*, 12(12), 155–164.

Brenner, H. (1962). "The diffusion model of longitudinal mixing in beds of finite length. Numerical values." *Chem. Eng. Sci.*, 17(4), 229–243.

Buckingham, E. (1907). "Studies on the movement of soil moisture." *Bull. 38*, USDA, Bureau of Soils, Washington, DC.

Cavalcante, A. L. B., and Farias, M. M. (2013). "Alternative solution for advective-dispersive flow of reagent solutes in clay liners." *Int. J. Geomech.*, 10.1061/(ASCE)GM.1943-5622.0000164, 49–56.

Cavalcante, A. L. B., Ozelim, L. C. S. M., Swamee, P. K., and Rathie, P. N. (2013). "Explicit numerical iterative methods applied to the three-parameter infiltration equation." *Soils Rock, V*, 36(1), 129–133.

Cavalcante, A. L. B., and Zornberg, J. G. (2017). "Efficient approach to solving transient unsaturated flow problems. II: Numerical solutions." *Int. J. Geomech*, 10.1061/(ASCE)GM.1943-5622.0000876, 04017014.

Chen, G. J., and Gallipoli, D. (2004). "Steady infiltration from buried point source into heterogeneous cross-anisotropic unsaturated soil." *Int. J. Numer. Anal. Methods Geomech.*, 28(10), 1033–1055.

Chen, J.-M., Tan, Y.-C., and Chen, C.-H. (2003). "Analytical solutions of one-dimensional infiltration before and after ponding." *Hydrol. Processes*, 17(4), 815–822.

Chen J.-M., Tan, Y.-C., Chen, C.-H., and Parlange, J. Y. (2001). "Analytical solutions for linearized Richards eqution with arbitrary time-dependent surface fluxes." *Water Resour. Res.*, 37(4), 1091–1093.

Cleary, R. W., and Adrian, D. D. (1973). "Analytical solution of the convective-dispersive equation for cation adsorption in soils." *Soil Sci. Soc. Am. J.*, 37(2), 197–199.

Dell'Avanzi, E., Zornberg, J. G., and Cabral, A. (2004). "Suction profiles and scale factors for unsaturated flow under increased gravitational field." *Soils Found.*, 44(3), 79–89.

Fityus, S. G., and Smith, D. W. (2001). "Solution of the unsaturated soil moisture equation using repeated transforms." *Int. J. Numer. Anal. Mech. Geomech.*, 25(15), 1501–1524.

Gardner, W. R. (1958). "Some steady-state solutions of the unsaturated moisture flow equation with application to evaporation from a water table." *Soil Sci.*, 85(4), 228–232.

Gershon, N. D., and Nir, A. (1969). "Effect of boundary conditions of models on tracer distribution in flow through porous mediums." *Water Resour. Res.*, 5(4), 830–840.

Ghotbi, A. R., Omidvar, M., and Barari, A. (2011). "Infiltration in unsaturated soils—An analytical approach." *Comput. Geotech.*, 38(6), 77–782.

Hillel, D. (2004). *Introduction to environmental soil physics*, Elsevier Science, San Diego, 494.

Hogarth, W. L., and Parlange, J. Y. (2000). "Application and improvement of a recent approximate analytical solution of Richards' equation." *Water Resour. Res.*, 36(7), 1965–1968.

Hogarth, W. L., Parlange, J. Y., and Braddock, R. D. (1989). "First integrals of the infiltration equation: 2. Nonlinear conductivity." *Soil Sci.*, 148(3), 165–171.

Hogarth, W. L., Parlange, J. Y., and Norbury, J. (1992). "Addendum to 'First integrals of the infiltration equation.'" *Soil Sci.*, 154(5), 341–343.

Huang, R. Q., and Wu, L. Z. (2012). "Analytical solutions to 1-D horizontal and vertical water infiltration in saturated/unsaturated soils considering time-varying rainfall." *Comput. Geotech.*, 39, 66–72.

Jaiswal, D. K., Kumar, A., and Yadav, R. R. (2011). "Analytical solution to the one-dimensional advection-diffusion equation with temporally dependent coefficients." *J. Water Resour. Prot.*, 3(1), 76–84.

Lapidus, L., and Amundson, N. R. (1952). "Mathematics of adsorption in beds. VI. The effect of longitudinal diffusion in ion exchange and chromatographic columns." *J. Phys. Chem.*, 56(8), 984–988.

Lindstrom, F. T., Haque, R., Freed, V. H., and Boersma, L. (1967). "The movement of some herbicides in soils. Linear diffusion and convection of chemicals in soils." *Environ. Sci. Technol.*, 1(7), 561–565.

Mason, M., and Weaver, W. (1924). "The settling of small particles in a fluid." *Phy. Rev.*, 23(3), 412–426.

Mathematica 10.0 [Computer software]. Wolfram Research, Inc., Champaign, IL.

Narasimhan, T. N. (2004). "Darcy's law and unsaturated flow." *Vadose Zone J.*, 3(4), 1059.

Ogata, A., and Banks, R. B. (1961). "A solution of the differential equation of longitudinal dispersion in porous media." *Professional Paper 411-A, A1-A9*, USGS, Reston, VA.

Parlance, M. B., Prasad, S. N., Parlange, J. Y., and Romkens, M. J. M. (1992). "Extension of the Heaslet-Alksne technique to arbitrary soil water diffusivities." *Water Resour. Res.*, 28(10), 2793–2797.

Parlange, J. Y., et al. (1997). "New approximate analytical technique to solve Richards equation for arbitrary surface boundary conditions." *Water Resour. Res.*, 33(4), 903–906.

Philip, J. R. (1960). "General method of exact solution of the concentration-dependent diffusion equation." *Aust. J. Phys.*, 13, 1–12.

Philip, J. R. (1969). "Theory of infiltration." *Advances in hydroscience*, V. T. Chow, ed., Vol. 5, Academic, New York, 215–296.

Rathie, P. N., Swamee, P. K., Cavalcante, A. L. B., de S. M. Ozelim, L. C. (2012). "Lagrange's inversion theorem and infiltration." *Int. J. Math. Comput. Phys. Electr. Comput. Eng.*, 6(7), 386–391.

Ross, P. J., and Parlange, J. Y. (1994). "Comparing exact and numerical solutions of Richards' equation for one-dimensional infiltration and drainage." *Soil Sci.*, 157(6), 341–344.

Sander, G. C., Parlange, J. Y., Kühnel, V., Hogarth, W. L., Lockington, D., and O'Kane, J. P. J. (1988). "Exact nonlinear solution for constant flux infiltration." *J. Hydrol.*, 97(3–4), 341–346.

Swamee, P. K., Rathie, P. N., de S. M. Ozelim, L. C., and Cavalcante, A. L. B. (2014). "Recent advances on solving the three-parameter infiltration equation." *J. Hydrol.*, 509, 188–192.

Tartakovsky, D. M., Neuman, S. P., and Lu, Z. (1999). "Conditional stochastic averaging of steady state unsaturated flow by means of Kirchoff transformation." *Water Resour. Res.*, 35(3), 731–745.

Terzaghi, K. (1943). *Theoretical soil mechanics*, John Wiley and Sons, New York.

Wang, Q. J., and Dooge, J. C. I. (1994). "Limiting cases of water fluxes at the land surface." *J. Hydrol.*, 155(3–4), 429–440.

Yeh, T. C. J. (1989). "One-dimensional steady state infiltration in heterogeneous soils." *Water Resour. Res.*, 25(10), 2149–2158.

Zhu, J., and Mohanty, P. (2002). "Analytical solutions for steady state vertical infiltration." *Water Resour.*, 38(8), 20-1–20-5.